Design of a Hybrid Renewable Plant-Based Hydrogen Production System Considering Electricity Market Prices in Finland

Lappeenranta–Lahti University of Technology LUT

Master's Thesis in Electrical Engineering

2024

Abolfazl Mirzaei

Examiner(s): Professor Behnam Mohammadi-Ivatloo

Doctoral Researcher Mohammad Seyfi

ABSTRACT

Lappeenranta–Lahti University of Technology LUT

LUT School of Energy Systems

Electrical Engineering

Abolfazl Mirzaei

Design of a Hybrid Renewable Plant-Based Hydrogen Production System Considering Electricity Market Prices in Finland

Master's thesis

2024

92 pages, 41 figures, 10 tables

Examiner(s): Professor Behnam Mohammadi-Ivatloo

Doctoral Researcher Mohammad Seyfi

Keywords: Optimization, Hydrogen, Renewable Plants, Electricity Market, Finland

The development of cost-effective and eco-friendly power to hydrogen systems is essential for achieving the lowest possible production cost of hydrogen. Ensuring a dependable and economical hydrogen supply becomes more challenging when dealing with fluctuating renewable energy sources. Hence, grid connection as one of the sources of input power along with a hybrid solar-wind source plus Finland electricity market prices is an approach considered in this research. This study aims to design a power-to-hydrogen system by conducting extensive simulations of several scenarios, primarily emphasising optimising hydrogen production and profitability. The research considers three scenarios, each combining distinct limitations and functioning characteristics, in order to evaluate their influence on system performance. The outcome is gained by engaging proper values of the components to design the size of the electrolyser, hydrogen tank, the volume of produced hydrogen, and revenues. Nevertheless, by comparing all scenarios the findings signify that in scenario I, producing hydrogen on a large scale substantially decreases the levelized cost of electricity and hydrogen, resulting in higher profitability. Still, it needs massive investment via private or governmental organisations. Moreover, by implementing constraints on the hydrogen sales and adjusting component capabilities, scenarios II and III represent a practical company setting with the lowest values of levelized cost of electricity, levelized cost of hydrogen, carbon intensity, and financial profit which are 0.048 €/kWh, 1.596 €/kg, 0.252 g_CO2/kWh, 126 M€ for scenario II and 0.034 €/kWh, 1.140 €/kg, 0.204 g_CO2/kWh, and 180 M€ for scenario III respectively. The findings indicate that the power-to-hydrogen system process meets environmental issues besides making profits for investors.

ACKNOWLEDGEMENTS

I would like to express my deepest gratitude to those who have supported and guided me throughout the journey of completing this thesis.

First and foremost, I am profoundly grateful to my academic supervisors, Professor Behnam Mohammadi-Ivatloo and PhD researcher Mohammad Seyfi, for their invaluable guidance, constructive feedback, and unwavering support. Their expertise and encouragement have been instrumental in shaping the direction and quality of this research.

I extend my sincere thanks to 3Flahs Finland Company for providing the resources and funds to conduct this study. The collaboration and insights from the company have significantly enriched the research and made it possible to explore practical applications in the field of power to hydrogen systems.

Lastly, I am deeply indebted to my wife for her endless patience, understanding, and encouragement. Her steady support and belief in me have been a constant source of strength and motivation, enabled me to overcome the obstacles encountered in this journey.

This thesis owes its existence to the vital contributions and solid support of these exceptional people. I express my appreciation to everyone for their immense support and encouragement.

Note: In this research, AI was utilized exclusively for enhancing language quality. Its role was limited to improving the overall readability of the text, ensuring clarity and coherence without influencing the substantive content or analytical processes of the study.

ABBREVIATIONS

AE	Alkaline Electrolyzer
AFC	Alkaline Fuel Cell
ANF	Annuity Factor
BS	Battery Storage
CAPEX	Capital Expenditure
CCS	Carbon Capture and Storage
CF	Capacity Factor
CI	Carbon Intensity
c/kWh	Cent per Kilowatt Hour
℃	Celsius
EM	Electricity Market
EU	European Union
EV	Electric Vehicles
FC	Fuel Cell
GHG	Greenhouse Gas
GtCO2eq/yr	Gigatons of Carbon Dioxide Equivalent per Year
GW	Gigawatt
GW_{ac}	Gigawatt Alternating Current
GW_{p}	Gigawatt Peak
HS	Hydrogen Storage
H_2	Hydrogen
IEA	International Energy Agency
IPCC	Intergovernmental Panel on Climate Change

LCOE	Levelized Cost of Electricity
LCOH	Levelized Cost of Hydrogen
Mt/y	Million Metric Ton per Year
MWh	Mega Watt Hour
M€	Million Euros
NCES	National Climate and Energy Strategy
NPC	Net Present Cost
OPEX	Operational Expenditure
PEM	Proton Exchange Membrane Electrolyzer
PEMFC	Proton Exchange Membrane Fuel Cell
P2X	Power-to-X
PtH	Power to Hydrogen
PWA	Piecewise Affine
PV	Photovoltaic
RES	Renewable Energy Sources
SOC	State of Charge
SOEC	Solid Oxide Electrolyzer
TWh	Terawatt Hour
TJ	Terajoule
t/a	Ton per Annum
UNSDG	United Nations Sustainable Development Goal
VRES	Variable Renewable Energy Sources
VtG	Vehicle to Grid
€/MWh	Euro per Megawatt Hour
VAT	Value-Added Tax

Table of contents

1 Introduction

The escalating and observable impacts of global warming are prompting a rapid shift toward carbon neutrality, and hydrogen (H_2) is gaining prominence as a crucial driver in the shift toward sustainable energy. Its array of advantages has gathered heightened interest from diverse stakeholders, prompting numerous countries to concentrate on shaping and refining their hydrogen strategies. Hydrogen, as the most plentiful element globally, possesses greater mass-energy density than hydrocarbons, generates water vapour when burned, is not poisonous, and can be produced in an environmentally friendly manner by electricity and water. The transformative potential of hydrogen in the energy system is widely acknowledged, promising substantial climate benefits. Functioning as a chemical carrier, hydrogen offers large-scale and seasonal energy storage, enhancing the flexibility of energy system management and optimizing the total system. The production of renewable hydrogen is poised for significant expansion in the forthcoming decades and wind and solar are one of the most substantial sources of producing green hydrogen.

The technique of modelling hybrid renewable sources such as solar-wind systems is critical for establishing crucial components in system design while taking into account unique characteristics and limits. This modelling approach normally addresses essential parameters such as scope standards, environmental statistical features, battery self-sufficiency function, and annual cost analysis. However, multiple studies have stressed various modelling methodologies for hybrid system components. In solar system modelling, the emphasis is frequently on outputs impacted by solar cell efficiency and solar radiation [1][2] in contrast, the modelling of wind turbines involves the consideration of additional factors, including mechanical power, power coefficient, wind velocity, tip-speed-ratio, and stall behaviour [1].

The durability of solar modules and wind turbines is strongly related, resulting in a longer lifespan when incorporated into a hybrid system, improving total longevity and dependability [3]. Nonetheless, climatic variables play an important role in the design of hybrid solar-wind systems since both components work in distinct weather. Solar modules thrive under intense solar radiation, while wind turbines require appropriate wind velocities for optimal performance [4].

Gökçek and Kale conducted a technological and economic evaluation for an independent hydrogen refuelling station not connected to the grid in Turkey, utilizing solar and wind energy sources. They utilized commercial software to model the system, optimizing it to fulfill a daily 125 kg hydrogen need. The optimum plant design incorporated an energy storage system using batteries as a reserve, resulting in an achieved 7.526 $/kg levelized cost of hydrogen (LCOH). While the utilization of business software offers a computational structure. For simulating plant operations, this method may pose limitations in modelling systems and understanding the employed methods [5].

Ibáñez-Rioja et al. presented optimization findings showing that the most cost-effective configuration for a plant in Southeastern Finland until 2035 is wind power generation with the water electrolyser. The LCOH falls from 2.34 €/kg in 2020 to around 1.72 €/kg in 2040, with the goal of attaining less than 2 €/kg by 2030. While solar PV and battery storage (BS) are not commercially viable until 2035-2040, their combination doubles the electrolyser's total full-load hours and hydrogen output. The improved system control demonstrates that the BS serves as a short-term storage option, guaranteeing that the electrolyser runs at a low load during periods of insufficient solar PV and wind power generation [6].

In comparison, Sorrenti et al. explored the influence of the capacity ratio between renewables and electrolysers in a grid-connected Power-to-X (P2X) system on its economics and carbon intensity (CI), using real data from Denmark's GreenLab Skive industrial park. The study looked at four different scenarios of solar and wind energy, taking into account long-term sustainability and economic feasibility. Key conclusions include the use of renewables in P2X technology for lowering emissions and establishing economic viability. A combination of wind, solar PV, and a grid-connected electrolyser is shown to be the highest economically efficient and low in carbon emissions [7].

This research, investigates a setup dedicated to optimal renewable hydrogen generation, focusing on minimizing the LCOH and maximizing hydrogen output. BS and grid are used in times of deficit renewable power to support the alkaline electrolyser (AE). Through simulation using GAMS software, electricity market prices in Finland, AE, and fuel cells (FC) with the integration of solar PV and wind turbine sources are considered. Building upon this methodology, the present thesis has improved the techno-economic models to enhance the accuracy and reliability of optimal hydrogen production in Finland.

By incorporating the Finnish electricity market prices into the research framework, the study aims to identify optimal strategies for decision-making regarding when to produce hydrogen and when to sell electricity. This optimization process is driven by the objective function of maximizing revenue generation resulted via selling electricity and hydrogen, finally leading to enhanced profitability for stakeholders involved in the hydrogen production process.

One significant aspect of this research is its pioneering nature within the context of Finland. Before this study, there had been a notable absence of similar research endeavours focused on the Finnish electricity market and its implications for hydrogen production. As such, this study fills an important gap in the existing literature and contributes to a more comprehensive understanding of Finland's energy landscape. By leveraging sophisticated software tools to optimize the entire system, this research promises to shed light on the complexities of Finland's electricity market dynamics. This holistic approach not only benefits stakeholders directly involved in hydrogen production but also provides valuable insights for policymakers, energy analysts, and other relevant stakeholders interested in the sustainable development of Finland's energy sector.

An extensive and analytical review of relevant literature was conducted in Chapter 2 to establish a robust theoretical framework and effectively address the research concerns while aligning with the objectives.

Chapter 3 outlines the methodology, detailing the model with mathematical equations to simplify system modelling and showcase component integration. This section serves as a guide, explaining model development step-by-step and providing a rationale for chosen techniques and parameters. Overall, it offers a concise overview of the methodology, laying the groundwork for subsequent analyses.

Chapter 4 entails the simulation phase, where the GAMS software was employed to optimize the model using data sourced from 3Flash Finland Company and reputable publications. This section focuses on evaluating the model's performance in maximizing both hydrogen production and revenue for stakeholders.

In Chapters 5 and 6, the study's outcomes are presented and thoroughly examined. The results are carefully analysed, leading to discussions on their significance and potential implications. Finally, in the concluding segment, recommendations are made, suggesting

suitable values from both economic and environmental standpoints to effectively meet the requirements and preferences of the stakeholders involved.

Ultimately, it should be noted that this research endeavour has been funded by 3Flash Finland Company with the specific aim of evaluating the feasibility and effectiveness of an optimal hydrogen production project in Finland.

2 Literature review

This chapter seeks to provide a concise overview of optimizing hydrogen production using renewable energy sources (RES), particularly solar and wind, in combination with the grid. It also considers the electricity market in Finland to analyse market prices and ensure the efficiency and cost-effectiveness of hydrogen production. Additionally, this section will present key metrics of the power to hydrogen system to offer a better understanding of the current state of hydrogen production.

2.1 Green hydrogen overview

In recent times, a substantial body of literature has emerged addressing the symbolic rise in environmental concerns linked to the escalation of global average temperatures, the surge in greenhouse gas (GHG) attentions, and the elevation of GHG release points. This is underscored by numerous reports highlighting climatic imbalances worldwide, with particular attention to coral reefs being recognised as the initial planetary ecosystem facing the threat of substantial destruction [8]. The Paris Agreement marked a pivotal milestone in establishing a cohesive energy policy that emphasised the role of GHG emissions from fossil fuels as a major factor in global warming. It classified the utilisation of fossil fuel energy sources as a significant peril to the future of human existence [9]. Leaders and societies worldwide, as known by the Intergovernmental Panel on Climate Change (IPCC), have acknowledged the imperative for a shift toward sustainable energy systems. This has heightened interest and concentration on avenues that prioritise energy storage technologies and renewable energy systems [10].

Hydrogen has been acknowledged as a key energy pathway for realizing a sustainable transition in energy storage and utilization. This recognition aligns with the growing utilization of various RESs within a developmental framework established by the IEA [11]. Hydrogen plays a crucial role as a raw material in industrial processes and holds promise as a potential clean fuel [12]. The primary approach for generating hydrogen is through fossil fuels, but this method leads to notable carbon emissions [13]. To mitigate the detrimental effects of utilizing fossil fuels on the atmosphere, individuals' health, and climate, it is

imperative to produce hydrogen from RESs employing environmentally friendly techniques. Consequently, there has been a significant global concern in hydrogen production from sustainable sources such as water [14], photovoltaic (PV) [15], biomass [16], wind, oceanic, and hydropower [17].

The European Union (EU) seeks to employ hydrogen to facilitate the shift from fossil fuel-oriented resources to one based on renewable sources. Storage technologies, including batteries and hydrogen, play a central role in realizing this transformative shift [10]. The worldwide creation of pure hydrogen until the end of 2021 is approximately 75 Mt/y, along with an additional 45 Mt/y when combined with other gases. This represents approximately 3% of the whole universal energy demand, which is roughly equivalent to Germany's annual energy consumption [18].

As it is shown in Figure 1 hydrogen serves as a flexible energy carrier rather than directly serving as an energy source. It can be generated from various feedstocks and is applicable across a wide range of uses. Renewable electricity can undergo electrolysis to produce hydrogen, creating a connection between the growing renewable energy supply and challenging-to-electrify end uses. This linkage not only offers grid flexibility but also serves as a complement to substitutes such as demand response, vehicle-to-grid, and batteries in the realm of smart electrification [18].

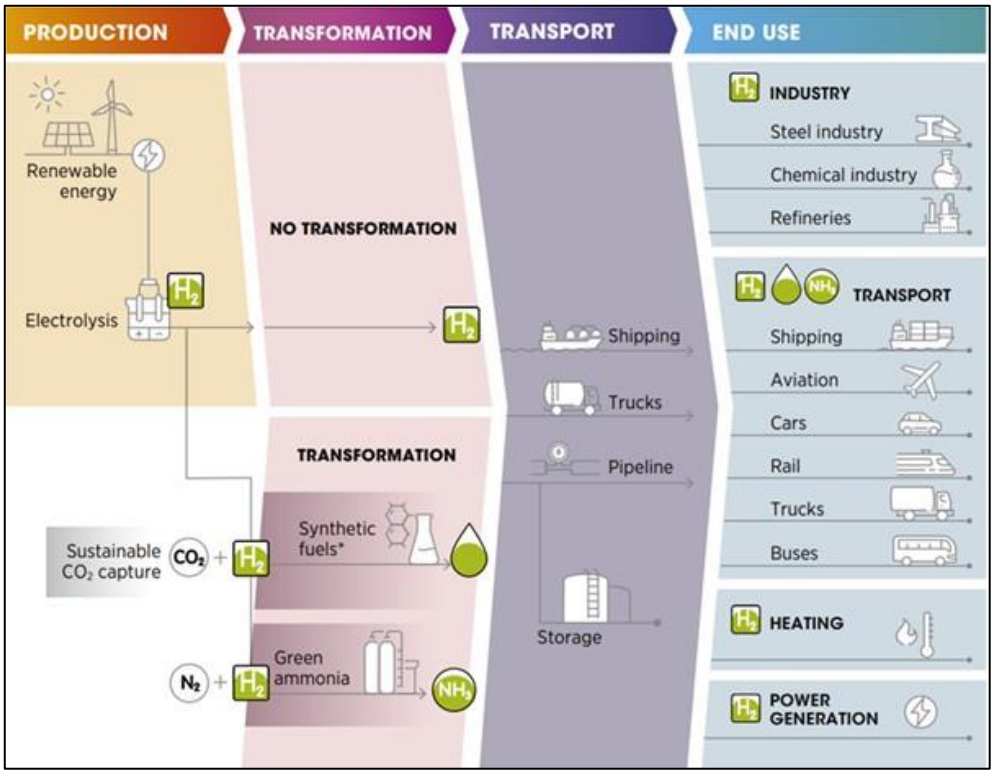

Figure 1. The production, conversion, and utilization of green hydrogen [18].

2.1.1 Types of hydrogen

Three primary categories of hydrogen production are Gray Hydrogen, Blue Hydrogen, and Green Hydrogen.

Gray Hydrogen: currently the most economically efficient method of hydrogen production, relies on finite fossil fuel resources, leading to substantial carbon dioxide emissions during the manufacturing process. Despite its cost-effectiveness, this approach is not a sustainable long-standing answer because of its significant contribution to GHG emissions. Globally, the main sources of hydrogen production, particularly coal and natural gas, are major contributors to the production of gray hydrogen [19].

Blue Hydrogen: it relies predominantly on natural gas for production, but it distinguishes itself from gray hydrogen by incorporating the capture and storage of carbon emissions during the process. Unlike gray hydrogen, which does not address carbon emissions, blue hydrogen is considered a low-carbon option. The production process for blue hydrogen

closely resembles that of gray hydrogen, involving vapour methane restoration to extract hydrogen from natural gas [20].

Green hydrogen: it stands as a sustainable and dependable energy source capable of competing with traditional fossil fuels and has the potential to significantly augment renewable energy production capacity. It can be generated through water electrolysis, wherein electricity is used to separate water into hydrogen and oxygen. This process can be accomplished with zero GHG releases, given that the electricity used to drive the electrolysis is sourced entirely from renewable energy [21].

2.1.2 Production methods and technologies of green hydrogen

While renewable sources currently contribute only a minor portion to the global hydrogen output, the associated technologies are not yet commercially mature, and their production costs are not competitive compared to fossil fuels. Despite these limitations, the sector remains promising, with a strong research emphasis and a pressing need to minimize dependency on fossil fuels. In the near prospect, the percentage of renewable tools is likely to expand, and it is expected to prevail over traditional technologies in the long run [22] [23].

Electrolysis: Electrolysis stands out as one of the most effective approaches for producing hydrogen from water. This method involves utilizing electricity to separate hydrogen and oxygen from water. Implemented within a device called an electrolyser, this endothermic process facilitates the separation of water into its constituent gases [24][25][26]. The material used for the membrane, which serves as a separator between the anode and cathode, determines the electrolyzer's classification [24]. The three main categories of electrolyser membranes are alkaline electrolysers (AE), solid oxide electrolysers (SOEC), and proton exchange membrane electrolysers (PEM) [27].

Water electrolysis is an environmentally beneficial method of producing high-quality hydrogen for use in a variety of applications, including ammonia synthesis and FCs. With a productivity range of 60 to 81%, water electrolysis is economically superior to many other clean skills [9].

Thermolysis: It requires heating water at temperatures above 2500 degrees Celsius to convert it into hydrogen and oxygen. This technique depends on the considerable Gibbs free

energy of water at these extreme temperatures, which allows the separation of hydrogen from the equilibrium mixture [28].

Photo-electrolysis: The process of photo-electrolysis entails splitting water into hydrogen and oxygen through the use of a semiconductor electrode that absorbs visible light [29]. Hydrogen and oxygen are gained by breaking down the water which is influenced by absorbing sunlight from semiconductors [22].

2.1.3 Current and future capacity of green hydrogen

At the end of 2021, nearly half of the global hydrogen production came from natural gas 47%, followed by coal 27%, oil as a by-product 22%, and only a minor portion around 4% from electrolysis. In the same year, the global average renewable share of electricity was approximately 33%, highlighting that only about 1% of the globe's hydrogen supply was generated using renewable energy bases [18].

Between 2022 and 2027, the worldwide renewable capacity designated for hydrogen production is poised to increase dramatically by a factor of 100, providing significant opportunities for reducing carbon emissions in industry and transportation. The implementation of policies and targets in more than 25 countries is expected to result in the establishment of 50 gigawatts (GW) of wind and PV capacity specifically directed towards hydrogen production during the abovementioned time. This expansion is distributed across diverse geographic regions, with China leading the way, followed by Australia, Chile, and the United States. Together, these four markets contribute to roughly two-thirds of the total dedicated renewable capacity for hydrogen production [30].

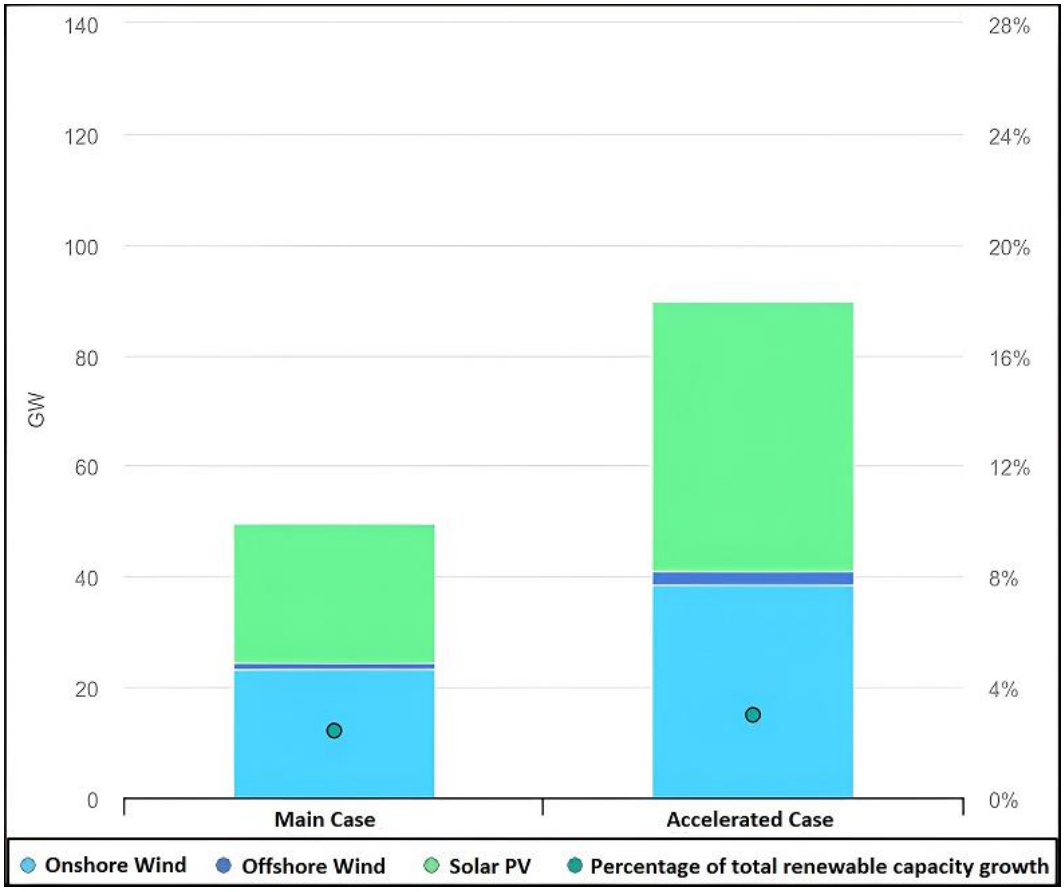

Figure 2. Combined renewable capacity allocated for hydrogen production in the primary and accelerated scenarios on a global scale from 2021 to 2027 [31].

Figure 2 illustrates the contribution of the onshore wind, offshore wind, and solar PV capacity were 23.2 GW, 0.1 GW, and 26.4 GW in 2021 respectively for producing hydrogen, supporting a total renewable capacity growth of 2.4%. Conversely, by 2027, the total capacity growth increased to 3%, with onshore, offshore wind and solar PV reaching 38.6 GW, 2.4 GW, and 48.7 GW respectively [31].

2.1.4 Cost of producing green hydrogen

Enthusiasm for hydrogen is guided by the declining fees of renewable energy and electrolysers [32]. In addition, there is backing for the expansion of conventional methods of hydrogen production from fossil drives, incorporating carbon capture and storage (CCS). However, questions arise about the compatibility with global decarbonization objectives due to residual CO2 emissions after CCS. Carbon capture is an established technology employed

across various industries, yet the costs and the potential for reducing CO2 emissions vary significantly and are challenging to quantify in certain instances. The quantity of captured CO2 is influenced not just by the method and stage in the development where CO2 is arrested but also by the subsequent utilization of the collected CO2 [33].

The expenditures accompanying carbon avoidance in CCS are contingent on the capture process type. These costs encompass the transportation and storing of the captured CO2, which are highly dependent on the exact plant. They also involve the reviewing and observing of capture values and potential leaks of upriver methane or CO2. Generally, price estimations for CCS may not consistently consider all these diverse components [34].

On the contrary, generating hydrogen through electrolysis powered by renewable energy is emission-free. The expense linked with producing hydrogen using renewables is primarily influenced by the cost of the input electricity, along with the principal charge and load issue of the electrolyser. As the scale and implementation of renewables and electrolysers increase, the cost of this hydrogen generation method is anticipated to decrease [35][36].

Green hydrogen is generated through electrolysis utilizing RES priced at 6 $ (5.09 €) per kilogram in the year 2020 [37]. Under the mean European wind energy efficiency, the forecast indicates a cost of 2.50 $ (2.12 €) per kilogram in 2030. Nevertheless, the recent substantial reductions in the cost of RES electricity present new possibilities [38].

The manufacturing costs of electrolysers are estimated to experience a significant decline with the widespread deployment of such systems [39]. In 2019, the capital cost of AEC electrolysers ranged from 500 $ to 1400 $ per kilowatt, and it is expected to decrease to a range of 400 $ to 850 $ per kilowatt by 2030. For PEM electrolysers, the capital cost was between 1100 $ and 1800 $ per kilowatt in 2019, with projections indicating a range of 650 $ to 1500 $ per kilowatt by 2030 [9]. Even so, there have been reports of lower capital costs.

The recent price reductions in solar PV and wind power generation have resulted in a fall in the cost of hydrogen synthesis via electrolysis. Between 2010 and 2019, capital expenditures for solar PV systems dropped by 79%, while onshore wind turbines fell by 24%. This results in lower average costs for energy generation during the life of the facility. The levelized cost of electricity (LCOE) for PV projects was 35 $/MWh in 2020 and is expected to drop to 20 $/MWh by 2030. For wind, the equivalent numbers are 33 $/MWh and 31 $/MWh [40].

Based on information from the Hydrogen Council and McKinsey & Company, the LCOH from solar in Europe was approximately 7.5 $/kg$H_2$ in 2020. In comparison, the corresponding values for offshore wind and onshore wind were notably lower at 4.4 $/kg$H_2$ and 4.2 $/kg$H_2$, respectively [41].

According to Ou Tang et al., wind speed has a greater effect on green hydrogen costs than sun radiation. In Stockholm, they identified a LCOH of roughly 3.5 €/kg H_2 for on-grid facilities incorporating both wind and solar power, whereas the LCOH for grid-connected solar plants alone was around 7.2 €/kg H_2. Their analysis also revealed that in facilities without grid connection, the LCOH was nearly twice as high as in on-grid scenarios [42].

2.1.5 Hydrogen condition in Finland

In Finland, the existing capacity for dedicated hydrogen production is approximately 140,000–150,000 t/a (4.7–5.0 TWh), and almost the entire production, nearly 99%, is obtained from fossil fuels. Projections suggest that the overall production could increase to nearly 175,000 t/a by the year 2030 [43].

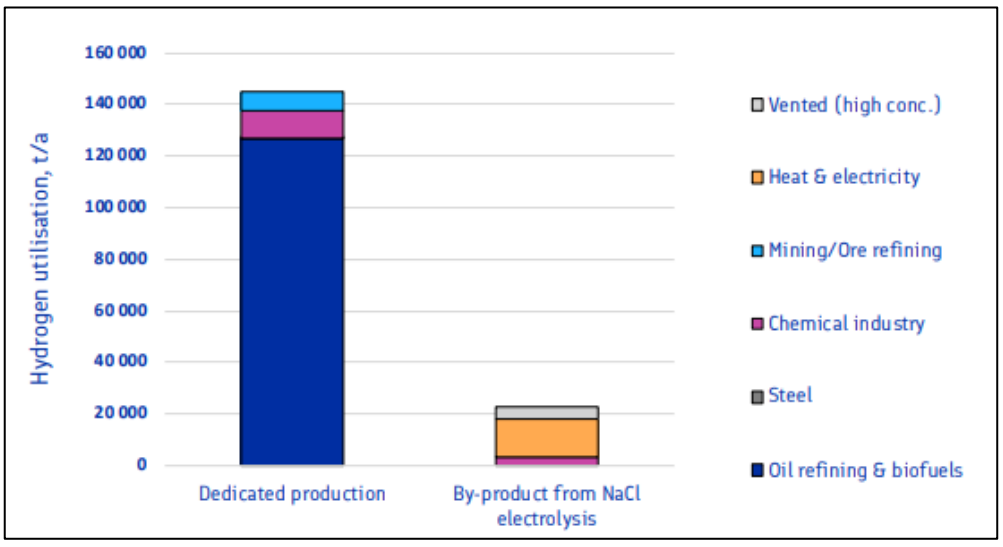

Figure 3. Hydrogen production in Finland in 2020 [42].

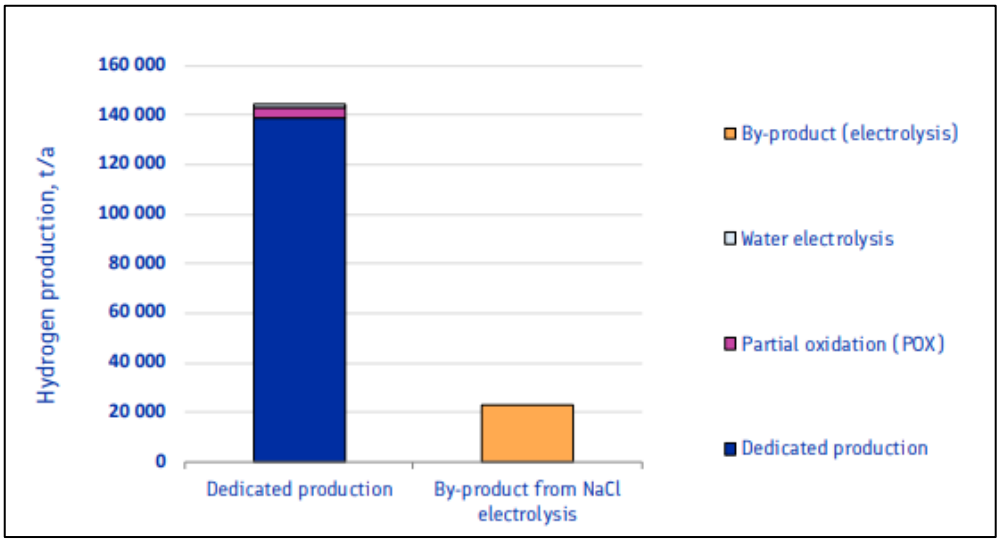

Figure 4. Hydrogen utilization in Finland in 2020 [42].

Figure 5 illustrates the distribution across geographical locations of hydrogen production plants in Finland and their respective annual hydrogen production capacities. The country currently has only a dozen dedicated hydrogen production sites. Concerning the present utilization sites of hydrogen, they are primarily situated in the southern to southeastern regions of Finland. In contrast, the anticipated locations for new wind power production are predominantly in the northern areas [42]

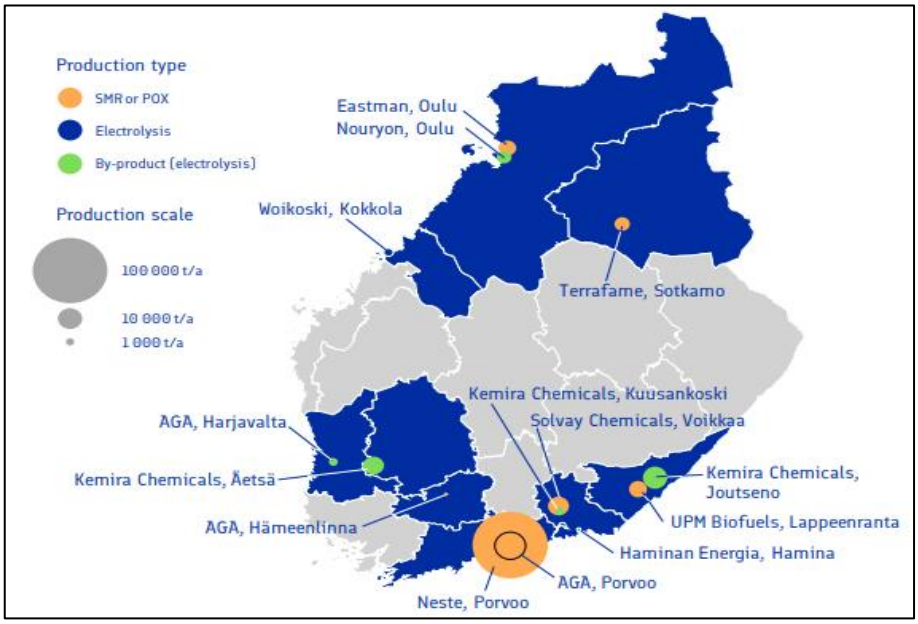

Figure 5. Producing and utilizing hydrogen by location in Finland [42].

With direct electrolysis contributing to less than 1% of hydrogen production and the majority sourced from fossil fuels, 88% of the total is utilized in oil purifying and biofuel construction, notably by the Porvoo Neste refinery, the principal individual hydrogen consumer. Hydrogen finds application in industrial hydrogen peroxide production (7%) and the mining industry (5%). Presently, only a limited quantity is employed in the steel industry primarily for oxidation prevention. Moreover, 22,000–24,000 tons per annum of hydrogen is generated as a by-product of sodium chloride electrolysis. Numerous tasks are underway to either enhance fossil-free hydrogen production or increase hydrogen utilization in industries. The 'SHARC' project, currently in the viability phase, Neste's Porvoo refinery in Finland plans to cut emissions from hydrogen generation by implementing electrolysis and carbon capture and storage technology [44].

2.2 Finland electricity market dynamics

This subsection will look at Nord Pool, a Nordic and Baltic power market exchange. Nord Pool arose from the Norwegian parliament's decision to de-regulate the power market. The decision to deregulate was reached in 1991, and the exchange began operations in Norway in 1993. It became international in 1996, when Sweden joined, followed by Finland and Denmark in 1998 and 2000. Expansion outside the Nordics began in 2005, expanding into Germany and then across the European continent. Nord Pool now provides a range of services, containing trading, settlement, clearing, and associated services to 360 firms in 20 countries [45].

Power in the Nordic and Baltic regions is dealt with across three markets: day-ahead (Elspot), intraday (Elbas), and regulating power (Real-time) at the Nord Pool power exchange. Nord Pool's initial concept, combining an Elspot marketplace with a regulation power market, was well-suited for dispatchable supply, particularly flexible hydropower. In contrast, the intraday market was specifically designed to provide less flexible generation technologies, which faced challenges in predicting generation accurately 12–36 hours ahead, as demanded by the Elspot market. Consequently, the intraday market acting a crucial character for producers employing variable generation, despite the day-ahead market having significantly higher daily trading volume [46].

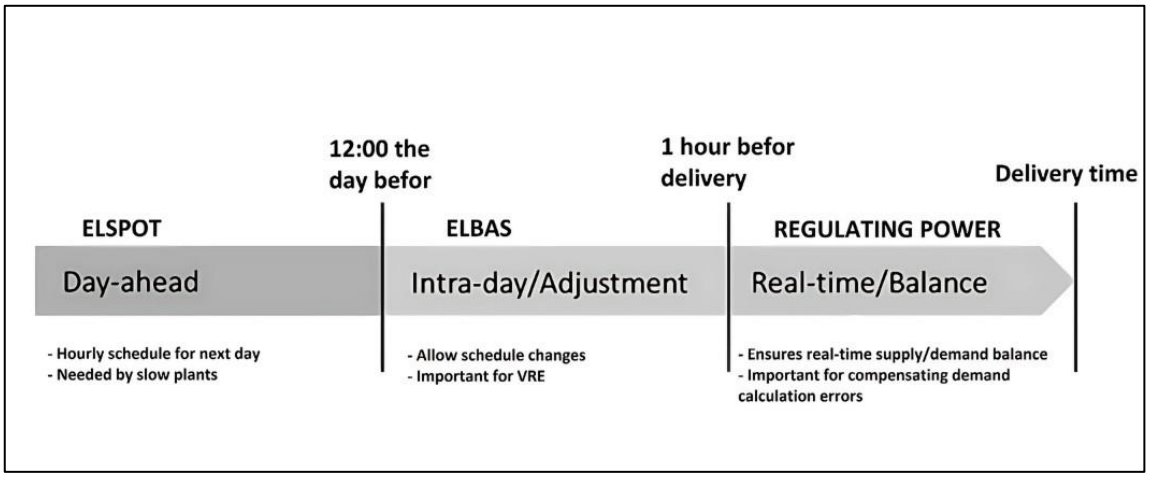

Figure 6. Overview of the Nordic electricity market structure [46].

2.2.1 Day-ahead Market

Elspot market primarily involves electricity retailers and major creation facilities as buyers, and large power plant owners as sellers. The market is divided into bidding zones, each managed by a transmission system operator in charge of observing grid overcrowding. Trading in the Elspot market involves physical power contracts for the following day, with a minimum requirement of 0.1 MW/h delivery. Participants must submit their buy and sell orders by 12:00 CET for the upcoming 24-hour period [47].

2.2.2 System price

A day-ahead system pricing for the following day is established based on the Elspot market's daily trading sequence. This transparent and consistent pricing applies to all market players and may be used as a baseline for fiscal power agreements. The system pricing is set hourly for the following day. Hourly demand and supply curves are created via aggregating all purchasing and selling offers for that hour, which serve as the foundation for these hourly system pricing.

When computing the system pricing, any limits on transmission capability concerning various environmental locations in the Nordic nations are ignored. In essence, the system pricing is based on the premise that the transmission capacity relating to the Nordic and

Baltic nations is limitless. Furthermore, the system price is known as the unconstrained market clearing price, because it balances the buying and selling actions in the exchange region without accounting for transmission restrictions [47].

2.2.3 Area price

The Nordic market comprises 15 bidding areas, with 1 in Finland, 4 in Sweden, 5 in Norway, 2 in Denmark, and one each for Baltic countries. The limitation of grid capacity poses a challenge to achieving a consistent price across the entire Nordic area. Area prices are determined by merging the demand and supply curves for each bidding zone, considering the transmission capacity amongst various districts. Although the explanation simplifies the process for a market with 2 zones, the underlying basis holds constant for the actual 15 bidding districts in the Nordic power marketplace [47].

2.2.4 Intra-day market

Intraday power trading is the continuous buying and selling of power on a power exchange that occurs on the day of delivery. A more detailed examination of certain market and physical processes is necessary, especially considering activities from the Elspot market settlement to the actual physical delivery. The interval between the actual delivery hour and the Elspot price agreement is lengthy, lasting up to 36 hours. Several variables contribute to changes in consumption and generation, necessitating the availability of trading opportunities for market participants throughout this period. The Elbas market is a nonstop real-time sensible marketplace for power trading that operates around the clock all year. It enables the matching of supply and demand up to one hour before delivery, resolving unanticipated events or differences that may occur after Elspot market activity [47].

Finland has a completely liberalized electricity market, which includes both wholesale and retail sectors. The wholesale trade industry works on an open platform that is available to all market players. Retail providers offer a variety of supply contracts, with prices decided by competitive forces. Customers have the ability to choose and transfer providers, and there are no restrictions or social tariffs limiting power rates. The Energy Authority is in charge of the regulatory components of Finland's electricity market, including transmission and

distribution networks, demand-side response, development and operation of generating, and energy storage. Corresponding to the Energy Authority's most recent market analysis, the power market remains generally competitive [48].

2.2.5 Electricity situation

According to Statistics Finland, the electricity production in Finland reached 69.1 TWh in the year 2022. The importation of electricity from Russia was discontinued in May 2022, leading to a 30% decrease in net electricity imports compared to the preceding year. On the other hand, the overall electricity usage in Finland for the year 2022 reached 81.7 TWh. Of this total, 85% was met through domestic production, while the remaining 15% was fulfilled by net imports of electricity [49].

Increased worries about the adequacy and elevated costs of electricity emerged in Finland. This led to a more frugal use of electricity compared to the norm, with a 6.2% reduction in electricity consumption, offsetting the decline in imports. In 2022, there was substantial growth in the domestic production of emission-free electricity: wind power production surged by 41%, and nuclear power production increased by 7% with the commencement of production at the Olkiluoto 3 nuclear power plant. Conversely, the production of district heat declined by six percent from the previous year [49].

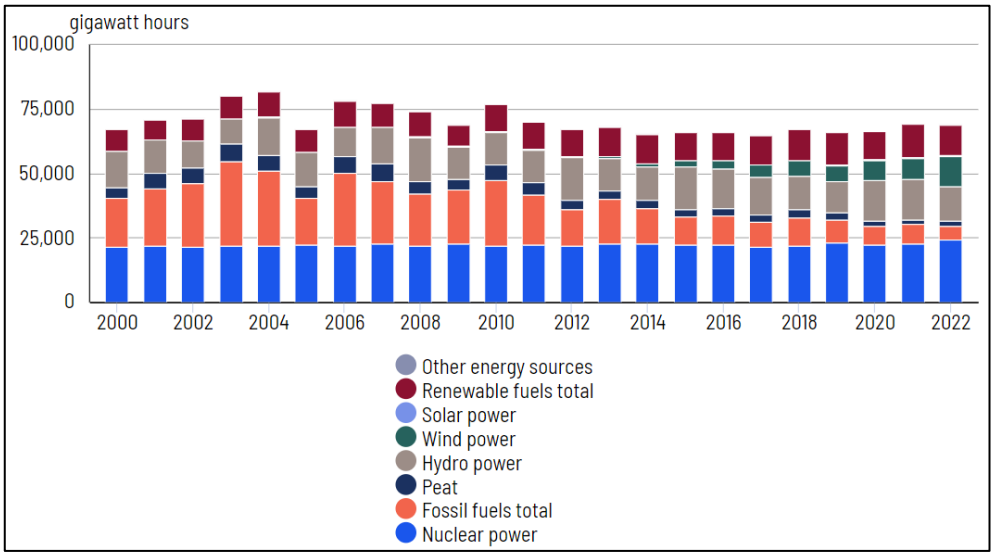

Figure 7. Electricity production by source in Finland [49].

Table 1. The exact value of the electricity production in Finland by source [49].

Unit: GWh	**2018**	**2019**	**2020**	**2021**	**2022**
Nuclear power	21,881	22,915	22,354	22,646	24,242
Fossil fuels total	10,876	9,096	7,278	7,572	5,348
Peat	3,25	2,821	1,998	1,952	2,032
Hydropower	13,137	12,246	15,669	15,624	13,337
Wind power	5,839	6,025	7,938	8,18	11,56
Solar power	90	147	218	298	392
Renewable fuels total	12,184	12,542	10,924	12,809	12,051
Other energy sources	274	258	216	244	229

At the start of 2024, the cost of electricity in Finland experienced an increase, surpassing 106 €/MWh. In the years 2021 and 2022, electricity prices surged across Europe due to a combination of factors, such as heightened heating demand during cold winters, elevated prices of natural gas and coal, and a reduction in wind power generation caused by low wind speeds. Consequently, Finland witnessed a nearly fourfold rise in electricity prices over the course of the year [50].

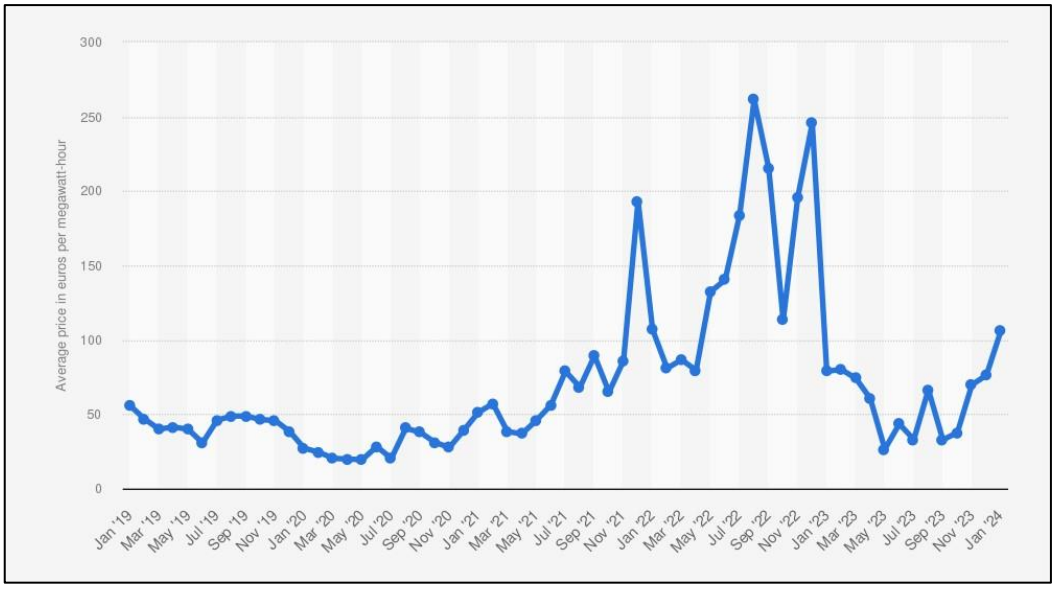

Figure 8. The mean monthly wholesale electricity price in Finland from January 2019 to January 2024 [50].

Furthermore, in the final quarter of 2022, households experienced the highest electricity costs. The average overall electricity price ranged from 20 to 34 c/kWh, varying based on the household's annual consumption. According to Statistics Finland, there was an increase of 23 to 26 percent from the preceding quarter and a surge of 41 to 49 percent from the same period in the previous year. In January 2023, the electricity price notably declined as stock market prices decreased [49].

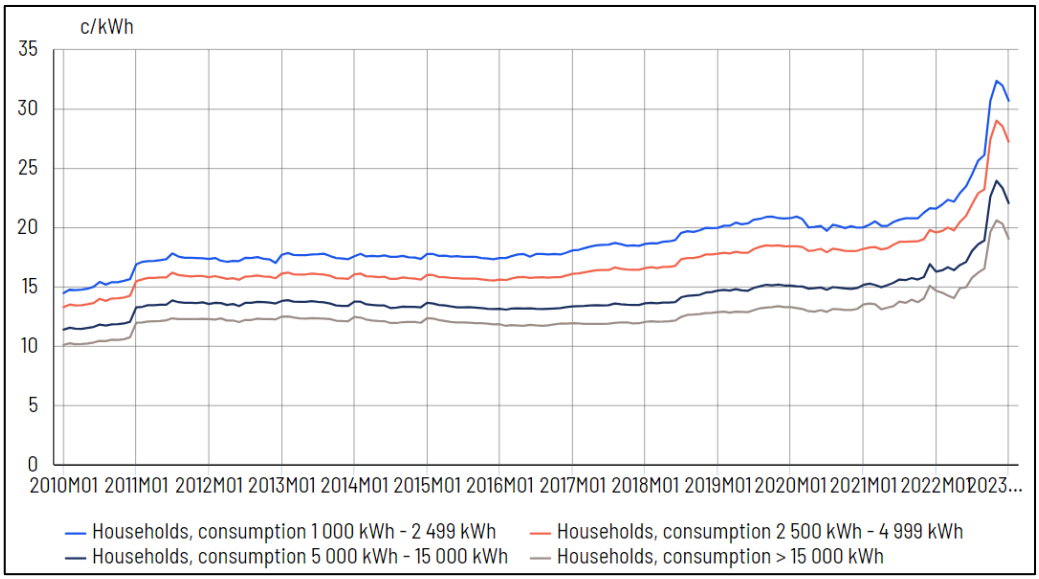

Figure 9. Electricity consumption price from January 2010 to January 2023 in Finland [49].

2.3 Renewable energy sources

The most substantial funder to global GHG production is the energy system, encompassing activities related to energy extraction, transmission and distribution, transformation, and storage. Human-induced GHG emissions have increased from 53 to 58 gigatons of carbon dioxide equivalent per year (GtCO2eq/yr.) amongst 2010 and 2019, significantly influencing worldwide climate shift [51]. The combustion of fossil fuels leading to air pollution poses a significant health burden and results in substantial societal costs [52] and the use of traditional fuels like wood and biomass for cooking has severe adverse effects, particularly in developing nations, with women and children bearing the brunt of these impacts. These

issues can be minimized by switching to renewable and sustainable energy sources and feedstocks within the energy system [53].

There are numerous options available to simultaneously decrease GHG emissions from the energy-industry system and address the increasing universal energy requirement. Some of these possibilities include enhancing energy efficiency, gradually eliminating the use of fossil fuels, and actively promoting renewable energy [51]. Ultimately, these measures could result in a full renewable energy system [54].

Solar, Wind, and hydropower are technologies that can serve as primary sources of renewable energy, enabling the accomplishment of decarbonization goals in the energy sector [55]. In recent years, the global expansion of PV and wind power has increased by 4% and 7%, respectively. Over the previous five years, the average gain has reached 13% for wind and 27% for solar [56].

In the last 18 months, European nations have implemented a greater number of policy and regulatory adjustments to streamline permitting than in the entire preceding decade. Although permitting has become a central policy emphasis in Europe to hasten the implementation of extensive wind and solar PV projects, the initial advantages are becoming apparent. However, the projected policy modifications are anticipated to exert a limited influence on renewable deployment in 2023 and 2024 when compared to other factors like the installation of small-scale residential and commercial solar PV systems [57]. Given the objective of this thesis to achieve optimal hydrogen production through solar PV and wind energy, the focus is primarily on assessing and analysing the concentration of these two renewable sources in Finland to facilitate the production of optimal hydrogen.

2.3.1 Solar PV

Solar PV stands out as the swiftest expanding power generation technology, offering more cost-effective electricity compared to fossil-fuel power plants in the majority of countries. It holds a crucial position in all pathways leading to a climate-neutral energy system. In the EU, solar PV accounted for 7% of electricity production in 2022, stemming from a cumulative installed capacity of 212 GW_p. The EU Solar Energy Strategy aims to achieve a four-fold increase from 2021 levels, reaching 600 GW_{ac} (720 GW_p) installed by 2030.

Solar PV prices remained relatively consistent in 2022, with mainstream modules priced at 0.35 €/W. However, a decline resumed in the first half of 2023, attributed to severe competition and an oversupply of components throughout the entire value chain. By September 2023, the price reached a historic low of nearly 0.22 €/W_p, posing profitability challenges in EU manufacturers' production efforts [58].

The increased deployment of renewable energy in Europe since 2021 has improved the economic consequences of the energy crisis. Inexpensive wind and solar PV sources are predicted to substitute around 230 terawatt hours (TWh) of costly fossil fuel generation between 2021 and 2023. This shift is expected to contribute to a decrease in wholesale electricity prices across all European markets [57].

2.3.2 Wind energy

Wind energy is a key RES in Northern Europe, continuously increasing its contribution to total electricity generation. Thanks to technological advancements and innovations, offshore wind energy is undergoing even more rapid growth and now constitutes a significant portion of overall electricity generation in several Northern European countries [59].

The construction costs for onshore and offshore wind farms are comparable, although the technologies employed differ. Wind generators are more cost-effective when compared to photovoltaic systems, and the costs can be further reduced through the implementation of high-efficiency power converters that can effectively operate based on atmospheric conditions [60].

Europe plays a vital part in the advancement of wind energy. In 2000, wind energy met 2.4% of the EU's electricity consumption, and this proportion rose to 10.2% by 2014 [61]. In 2022, the EU boasted a cumulative installed capacity of 204 GW, comprising 189 GW onshore and 16 GW offshore. A total of 16.2 GW was added in 2022, representing a nearly 50% surge compared to 2021. The new onshore capacity in 2022 was primarily installed in Germany, Sweden, and Finland, while offshore capacity saw significant additions in France and the Netherlands [58].

2.3.3 Renewable energy in Finland

Finland stands out as a global leader in harnessing RESs, with a noteworthy highlighting on bioenergy, including wood and wood-based fuels. The primary sources of renewable energy in Finland include bioenergy, derived from fuels produced by forest industry by-products and other wood-based sources, hydropower, wind power, and air and ground-source heat pumps. Additionally, solar electricity is gaining prominence, particularly in scenarios where on-site energy generation replaces grid-purchased energy. Solar heating is also employed as a supplementary component to the primary heating system [62].

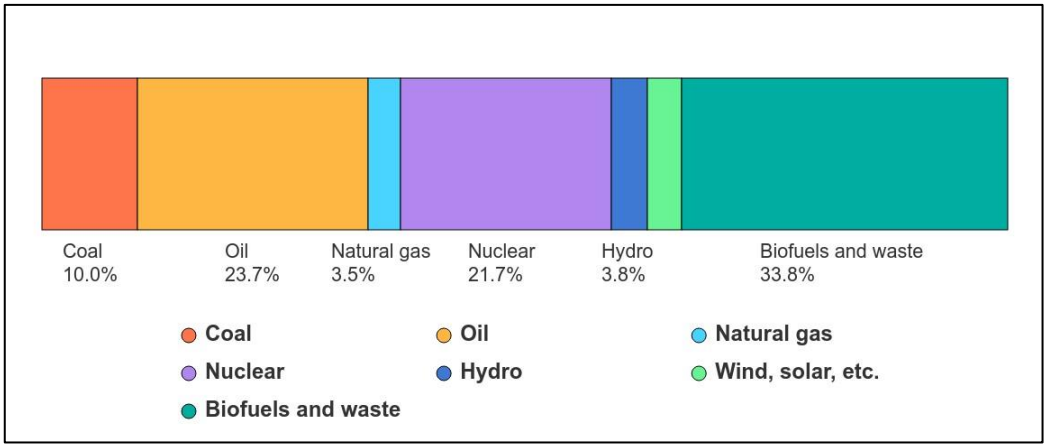

Figure 10. Total energy production in Finland in 2022 [63].

Table 2. The exact value of energy production in 2022 [63].

Source of energy	Unit	Amount
Oil	TJ	301,443
Coal	TJ	127,408
Natural gas	TJ	44,149
Nuclear	TJ	276,392
Hydro	TJ	48,571
Wind, solar, etc.	TJ	447,67
Biofuels and waste	TJ	429,316

According to preliminary data from Statistics Finland on energy consumption, the total energy consumption in 2022 was 1.29 million terajoules (TJ) (see Figure 11), reflecting a decrease of just under five percent compared to 2021. In 2022, wood fuels accounted for nearly 29% of the total energy consumption, making them the most widely used energy

source. Emission-free electricity generated from hydropower constituted 16.3% of the total electricity generation share in 2022 [62].

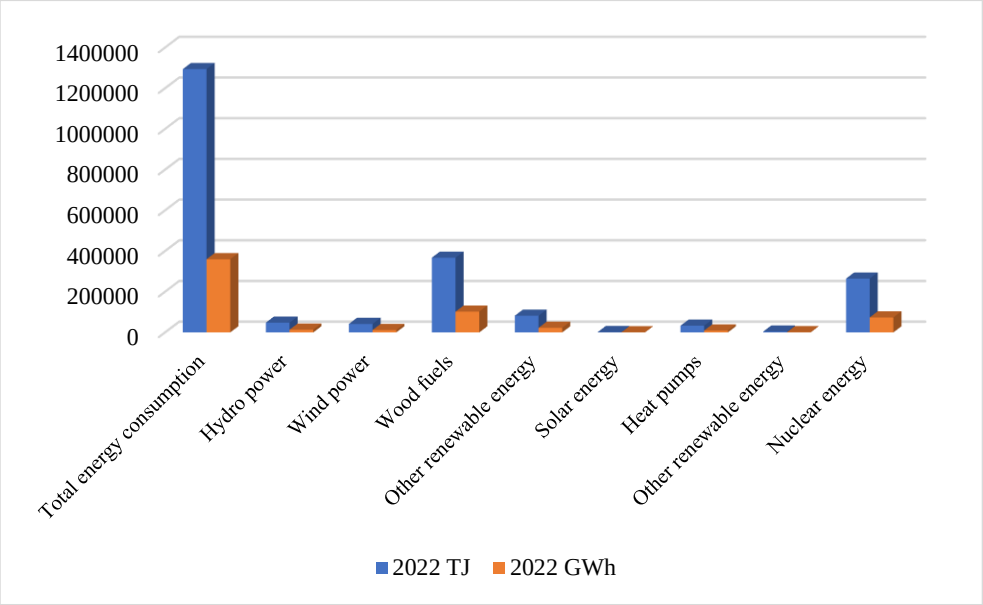

Figure 11. Finland's energy consumption by source in 2022 [64].

Table 3. The exact value of energy consumption in Finland in 2022 [64].

	Unit	
Source of energy	**TJ**	**GWh**
Total energy consumption	1,294,248	359,513
Hydropower	48,014	13,337
Wind power	41,615	11,56
Wood fuels	367,058	101,961
Solar energy	1,534	426
Biogas	2,98	828
Heat pumps	33,071	9,186
Nuclear energy	264,458	73,461
Hydrogen	878	244

The current installed capacity for hydropower is 3,200 MW, with no significant changes anticipated soon. As of the conclusion of 2022, Finland had installed 1,393 wind turbine generators, boasting a collective capacity of 5,677 MW. Wind power making witnessed a

notable 41% increase in 2022, achieving a record high of 11.6 TWh and accounting for 14.1% of the total electricity use [62].

Finland presently produces very little power from solar PV, with only 0.3 TWh expected by 2021. However, Finland aims to significantly increase its renewable energy generation, primarily focusing on wind and solar PV. According to the National Climate and Energy Strategy (NCES), it is projected that wind capacity will expand to a minimum of 6.8 GW by 2030, and PV capacity is predicted to reach at least 5.3 GW by 2030, a substantial increase from approximately 1 GW in 2022 [48].

2.3.4 Disadvantage of RES

The shift towards a 100% RE system involves an intricate procedure with diverse technical and economic challenges. To attain established objectives, multiple steps need to be undertaken concurrently, encompassing enhancements in energy effectiveness, reductions in prime energy utilization, and ultimately, the implementation of variable renewable energy sources (VRES) [65]. An increased share of alternating renewables such as solar and wind in the energy blend has a corresponding influence on grid stability, necessitating the flexible operation of traditional baseload power plants [66]. Furthermore, an increased proportion of VRES implies that instances of surplus or insufficient electricity production will occur more frequently. Consequently, it becomes imperative to incorporate short- and long-term energy storage solutions [67].

The grid is known to be able to support around 30% of VRES. The deployment of demand response technologies such as vehicle-to-grid (VtG), thermal storage, and different short-term storage methods can result in the integration of up to 80% of VRES. However, in order to completely incorporate VRES, the development of long-term energy storage devices is required. While hydropower and biomass are RESs that can be used in a decarbonized energy system, their availability might have limitations in some nations or areas. Moreover, excessive reliance on these resources to address the remaining 20% gap could be unsustainable [68].

Ultimately, the process of chemically converting surplus electricity into alternative fuels (Power-to-X) has emerged as a hopeful key. This technique not only operates as an energy transporter but also as a type of durable energy storage [69].

The power to hydrogen (PtH) process plays a role in assimilating variable renewable power generation and transforming surplus electricity into hydrogen. PtH systems, applicable both on- and off-grid, act as a strategy to prevent the wastage of excess electricity. They can also modulate the power demand they represent, offering load balancing, stabilization, or other services to the electricity grid. The rapid adjustment of power consumption is facilitated by the characteristics of hydrogen production through water electrolysis, allowing electrolysers to achieve full load operation in a matter of minutes, and even seconds [70].

2.3.5 Optimal hydrogen production by solar and wind

Certainly, stable hydrogen production is crucial in various engineering applications, including petroleum and petrochemicals. Addressing the challenge of meeting green and consistent hydrogen demand during uncertain inputs is vital. Achieving stable hydrogen production can be accomplished through various means. Firstly, incorporating a high-capacity hydrogen storage (HS) device is one approach [71]. The high investment associated with HS is attributed to its low density and compact volume, necessitating either high-pressure or low-temperature storage methods. Furthermore, hydrogen, being combustible and prone to spill, poses a safety issue [72].

Secondly, ensuring a continuous supply of renewable energy and utilizing battery energy storage to power the water electrolysis plant [73]. This approach proves to be a feasible solution in scenarios connected to the grid [74]. Nonetheless, in situations where there is no grid connection, economic obstacles emerge. The alternating spirit of RES creates issues, requiring the establishment of extensive BS infrastructure to ensure a consistently stable supply of hydrogen, especially for vital industries such as petroleum refining [41].

A meteorological study is required in solar-wind hybrid systems to determine the system's expected performance. Solar radiation, wind speed, wind direction, comparative moisture, and air temperature are all important meteorological characteristics in a hybrid solar wind system [75]. In contrast, a detailed assessment of load demand is a requirement for ensuring

electrical supply and minimizing yearly expenses [76]. Providing consistent weather-related data, completing a thorough study of load demand, and precisely calculating system requirements all contribute to a better system setup. This approach seeks to obtain an ideal arrangement while modelling a system by comparing energy production costs and performance across several systems, resulting in improved optimization analysis [77].

The optimization of PtH systems, which include both renewable energy and electrolyser producers, is critical for producing green hydrogen at the most cost-effective pace. Several studies in the following, back this statement.

Hassan et al. explained a specified assessment of searches on the generation of renewable hydrogen, examining technological, economic, environmental, and social factors [78]. Hofrichter et al. explored the ideal proportion between the electrolyser's installed capacity and renewable energy generators (including PV and wind power). The focus was on off-grid renewable energy systems, resulting in the lowest LCOH, 2.5 €/kg [79].

Scolaro and Kittner investigated the effectiveness of hydrogen generation related to a German offshore wind plant. The optimal LCOH is attained when the electrolyser capacity equals 87% of the wind farm capacity. demonstrated the economic benefits of participating in auxiliary service marketplaces [80]. PtH systems' economic affordability in Sweden was considered by Tang et al, with LCOH values ranging from 7.1 to 15.3 €/kg in off-grid situations and 3.5 to 7.3 €/kg in grid-connected states [81].

Scheepers et al. revealed that appropriate variables, such as electrolyser investment costs and power prices, have a considerable impact on the efficient model and process of an electrolyser [82]. María Villarreal Vives et al. noted the key factor impacting the LCOH is generally the cost of electricity needed to produce hydrogen. They especially looked at hydrogen costs under different energy rates, using a 10 MW PEM electrolyser [83].

After observing the articles and presenting related topics in the study, the next step is to delve into the core subject of this research. The upcoming chapter will provide a detailed explanation of the issue to demonstrate its functionality and significance thoroughly. This comprehensive analysis aims to illuminate the various aspects and implications of the subject, ensuring a clear understanding of its practical applications and relevance within the broader context of the study.

3 Methodology

This research target is to calculate production expenses associated with hydrogen technology. The emphasis is on evaluating production costs of optimal hydrogen generated by water electrolysis using RESs like solar PV and wind. In addition, the analysis focuses on the electricity market price in Finland to identify optimal days for cost-effective hydrogen production which involves assessing electricity prices in favourable times for hydrogen generation.

Furthermore, the potential for generating, converting, or storing hydrogen through this approach is explored. To mitigate the alternating nature of renewable sources, particular attention is given to grid connections, aiming for an enhanced and more reliable supply of hydrogen production, especially in light of the unpredictable climate in Finland.

In the end, this research explores hydrogen production taking into account economic and environmental conditions. To establish a framework that closely resembles reality, this study will use optimization design to evaluate the financial and technical operation of the integrated structure in diverse disturbances.

The study's major purpose and contribution are to propose the practicality of a combined renewable power system and grid to meet hydrogen demand. Photovoltaic cells, wind turbines, electrolysers, BS, HS, and FCs are the primary components of a renewable power system. The goal is to use GAMS software to model this framework as an integrated system, which will then be relaxed to estimate its economic, technological, and ecological profits.

3.1 System overview

This study presents a combined electricity and hydrogen production procedure designed to fulfill the hydrogen load demand through power supplied by renewable sources, including wind turbines and solar PV.

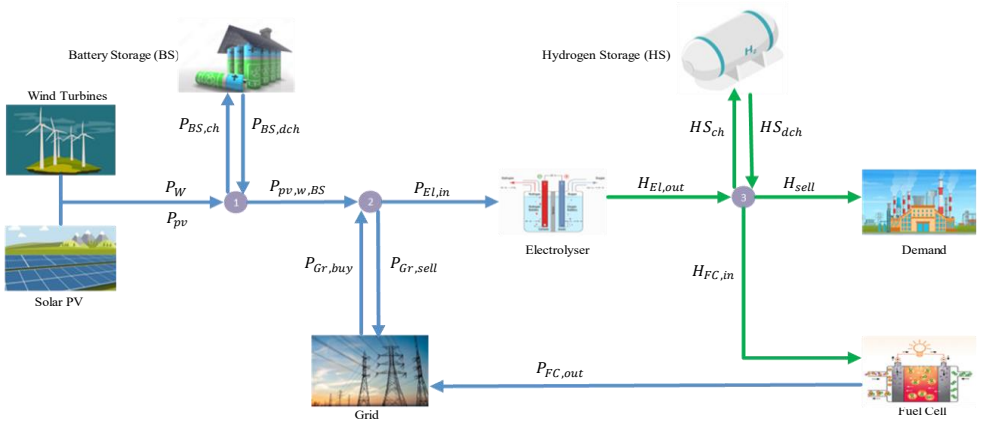

Figure 12. Power to hydrogen layout

Figure 12 depicts the operational concept of the system. To tackle the intermittency of these sources, BS, and the grid are employed to assist electrolysers during power deficits. When there is excess hydrogen, as a result of lower demand, the collected hydrogen in the reservoir releases to the FCs to generate power for later use, either for selling to the grid or for the potential of producing hydrogen.

3.2 Framework

The optimization's purpose is to comply with the hydrogen requirement at every time phase (t) within the specified time horizon (T) whenever reducing the PtH system's cost. The simulation covers hourly resolution in the one-year time frame, striking a balance between result accuracy and computational efficiency [84].

The primary contributions of the optimization method are as follows:

a) The required quantity of hydrogen to supply the demand

b) The climatic statistics indicating the accessibility of RES, represented by power creation in terms of capacity factor

c) The expense acquired for buying electricity from the grid (electricity buying fee) and the revenue generated by selling electricity back to the grid (electricity selling fee)

d) The technical and financial information for the entire machinery of the PtH structure, including wind turbines, solar PV, AE, BS, HS, and FC

And the decision variables include:

a) The dimensions of each component in the PtH system, including PV, wind, BS, AE, HS, and FC

b) Electrolyser and FC's operation state (on or off)

c) Electrolyser and FC's input and yield

d) Electricity traded by the grid (buy and sell)

e) Power and hydrogen charge and discharge rate of the BS and HS

f) Energy remained in the BS and HS

Design variables, denoted as (a), represent the dimensions of the established PtH tools, while operation variables, signified as (b) to (f), are calculated for separate time steps (*t*) within the time horizon (T).

The evaluated power sizes of the PV, wind, and AE modules were considered as constant variables, subject to constraints within minimum and maximum values, represented as follows (*j = PV, wind, AE*).

$$P_{j,rated,min} \leq P_{j,rated} \leq P_{j,rated,max} \quad (1)$$

Where $P_{j,rated}$ is the rated power, $P_{j,rated,min}$ is the minimum rated power, and $P_{j,rated,max}$ is the maximum measured power of the *j* modules.

Likewise, the measured energy sizes of the BS and HS approaches were restricted corresponding to the subsequent conditions (*j = BS, HS*).

$$E_{j,rated,min} \leq E_{j,rated} \leq E_{j,rated,max} \quad (2)$$

Where $E_{j,rated}$ is the rated energy, $E_{j,rated,min}$ is the minimum rated energy, and $E_{j,rated,max}$ is the maximum evaluated energy of the *j* elements. In equations (1 and 2), the lowest worth

scope was established as zero, implying that a particular technology is incorporated into the PtH procedure if the optimization method size rate is bigger than zero [85].

3.3 Power balance

Three distinct power equilibriums, As illustrated in Figure 12, need to be maintained across all time steps throughout the duration of the simulation. The initial power equilibrium (El in kW) applies to the solar PV, wind, and BS subsystem and was formulated by the following equation [85].

$$P_{PV}(t) + P_w(t) + P_{BS,dc}(t) = P_{PV,w,BS}(t) + P_{BS,ch}(t) \quad (3)$$

Where P_{PV} is the power produced by the solar plant, P_w is power generated by the wind turbines, $P_{BS,dc}$ is the power generated by the discharging of the BS, $P_{PV,w,BS}$ is the power leaving solar PV, wind, and BS subsystem, and $P_{BS,ch}$ is power made by charging the BS.

3.3.1 Solar PV modelling

Solar PV technology is used to transform solar energy into direct current (DC) electrical energy. The equations that describe the electricity produced by solar PV systems are as follows [86][87]:

$$P_{PV} = (A_{PV} \cdot n_{pv} \cdot \mathrm{G(t)} \cdot \eta_{PV}) \quad (4)$$

$$\eta_{PV}(t) = \eta_{PV,ref}\ (1- \alpha\ (T_c - T_{ref})) \quad (5)$$

$$T_c(t) = T_{amb}(t) + \mathrm{G(t)}(\frac{NOCT-25}{1000}) \quad (6)$$

Where P_{PV} is generated power by the panels in (kW), A_{PV} is the total area of the plant in (m^2), n_{pv} is the number of modules, G is the solar irradiation in (W/m^2), η_{PV} is solar PV panel efficiency which changes with the cell temperature, $\eta_{PV,ref}$ is modules efficiency under the reference circumstances in (%), α is temperature coefficient at the highest power in (℃), T_c is cell temperature in (℃), T_{ref} is the temperature at the test situation in (℃), T_{amb} is the ambient temperature (℃), and *NOCT* is the cell nominal operating temperature in (℃).

3.3.2 Wind turbines modelling

The coming formulas are employed to predict the production power of the wind turbine, represented as $P_w(t)$ [88][89].

$$P_w(t) = \begin{cases} 0 & V(t) < V_i \\ P_r & V_r \le V(t) < V_o \\ P_r \left(\frac{V(t)^3 - V_i^3}{V_r^3 - V_i^3}\right) & V_i \le V(t) < V_r \\ 0 & V(t) \ge V_o \end{cases} \quad (7)$$

Where P_r is wind turbine rated power in (kW), $V(t)$ is the location wind speed, V_i is the turbine wind speed (cut-in), V_r is the rated wind speed of the turbine, and V_o is the cut-out wind speed in (m/s). To calculate the wind turbine's hourly power generation, it is required to know the wind speed at the height of the turbine hub, which should drop inside the range of the turbine's cut-in and cut-out wind speeds for electricity generation.

To analogize the wind turbine hub speed, the power low is engaged as shown in equation (8) [90].

$$V = V_u \left(\frac{h}{h_u}\right)^{\beta} \quad (8)$$

Where V is the hub height wind speed in (m/s), h_u is the reference height in (m), h is the hub height in (m), V_u is the reference height of wind speed in (m/s), and β is the harshness factor influenced by the ground obstacle.

3.3.3 Interaction of the RE plants with grid

The second power equilibrium (El in kW) determines the collaboration of the PtH approach with the electrical network. Solar PV, wind farms, and FCs accompanying the electrical grid can meet the electrolyser's power requirements. Surplus renewable electricity can also be sold back to the grid.

$$P_{PV,w,BS}(t) + P_{Gr,b}(t) + P_{FC,out}(t) = P_{AE,in}(t) + P_{Gr,s}(t) \quad (9)$$

Where $P_{Gr,b}$ is the bought power from the grid, $P_{AE,in}$ is the input power of the AE, and $P_{Gr,s}$ is the power sold to the grid.

By considering the PV, wind, battery generation levels, and power prices, decision-makers may effectively choose the energy trading mode. The import and export of power in the grid (Gr) are limited by the market's capacity and the binary state that indicates the chosen trading mode. The next section provides an explanation of these limitations [91].

$$0 \leq P_{Gr,b}(\mathrm{t}) \leq P_{Gr,max} \quad (10)$$

$$0 \leq P_{Gr,s}(\mathrm{t}) \leq P_{Gr,max} \quad (11)$$

Where $P_{Gr,max}$ is the maximum power of the grid in (kW).

The third power equilibrium (H_2 in kg) refers to the hydrogen generation subsystem. It governs the electrolyzer's yield power as well as power transactions including HS in order to satisfy the end-user's demand. In addition, excess hydrogen in the low demand can be returned to the electricity by FCs.

$$H_{AE,out}(t) + H_{HS,dc}(t) = H_{HS,ch}(t) + H_{sell}(t) + H_{FC,in}(t) \quad (12)$$

Where $H_{AE,out}$ is the hydrogen output of the AE, $H_{HS,dc}$ is the HS discharging power, H_{sell} is hydrogen sell, and $H_{FC,in}$ is the input hydrogen of the FCs.

3.4 Electrolyser modelling

The electrolyser is the central component of the P2X plants. The AE has been utilized for several years due to the most developed machinery, reliability, and competitive cost [92] for generating hydrogen by water and electricity, relying on the oxidoreduction consequence within a cell with anode and cathode sections. AE operates at 80 ℃ and 35 bar following the proposed model of Ulleberg [93]. The productivity of the electrolyser is defined as the proportion of energy obtained in the form of hydrogen to the electrical energy supplied to the electrolyser [94]. Our model includes AE due to its advantages.

The mathematical representation for electrolyser modelling is given below. Equation (13) enables the calculation of the hydrogen produced by the electrolyser units, while equation (14) specifies the maximum allowable input power to the electrolyser [95].

$$H_{out} = \eta_H^{p2H} \cdot \varphi^{p2H} \cdot P_{in} \quad (13)$$

$$0 \leq P_{in} \leq U^{p2H} \cdot P_H^{p2H,max} \quad (14)$$

Where H_{out} is output hydrogen of the electrolyser, η_H^{p2H} is electrolyser efficiency, φ^{p2H} is the conversion factor of the power to hydrogen which is 33.3 *kWh/kg*, P_{in} is electrolyser input power, U^{p2H} is a binary variable for AE, and $P_H^{p2H,max}$ is the maximum power drawn by hydrogen-based energy.

3.5 Fuel cell modelling

Proton exchange membrane FC (PEMFC) is a sort of low-temperature FC that operates at temperatures ranging from 60 to 100 ℃. Notable features of PEMFC include their quick reaction to fluctuating loads, swift initialization, elevated power concentration, and minimized emissions. Also, PEMFC delivers consistent electrical power to a system under diverse operational and environmental circumstances [96]. However, compared to alkaline FC (AFC), PEMFCs are costly but advancements in PEMFC technology are driving down costs. The PEMFC is considered in this research.

Equation (15) determines the quantity of hydrogen utilized by FC units to generate electricity, factoring in performance efficiency. Equations (16) and (17) set constraints on both the hydrogen usage and power generation of FC units. It's important to highlight that binary variables are introduced in (18) to ensure the exclusive operation of these units [95].

$$H_{in} = \frac{P_{out}}{\eta_H^{H2p} \cdot \varphi^{H2p}} \quad (15)$$

$$0 \leq H_{in} \leq U^{H2p} \cdot H_H^{H2p,max} \quad (16)$$

$$0 \leq P_{out} \leq U^{H2p} \cdot P_{out,max} \quad (17)$$

$$U^{p2H} + U^{H2p} \leq 1 \quad (18)$$

Where H_{in} is the input hydrogen to FC, P_{out} is output power, η_H^{H2p} is FC efficiency, φ^{H2p} is the conversion factor of hydrogen to power 1/33.3 *kWh/kg*, $H_H^{H2p,max}$ is maximum power released by hydrogen-based energy, and $P_{out,max}$ is maximum output power.

3.6 BS and HS modelling

The hourly energy level of the storage system is determined by the charging and discharging processes taking place during that hour, as well as the residual energy from the previous hour. Each hour's charging and discharging numbers must adhere to the predetermined minimum and maximum criteria for storage. Additionally, it is important to note that every storage unit has a distinct energy storage capacity that must not be exceeded [97].

$$E_{BS}(t) = E_{BS}(t-1) + (\eta_{BS} \cdot P_{BS,ch}(t)) - \frac{P_{BS,dc}(t)}{\eta_{BS}} \quad (19)$$

$$Cap_{BS,min} \leq E_{BS}(t) \leq Cap_{BS,max} \quad (20)$$

$$0 \leq P_{BS,ch}(t) \leq P_{BS,ch,max}(t) \quad (21)$$

$$0 \leq P_{BS,dc}(t) \leq P_{BS,dc,max}(t) \quad (22)$$

Where E_{BS} is the BS energy in (kWh), $\eta_{BS,dc}$ are the efficiency of battery discharging in (%), $Cap_{BS,min}$ and $Cap_{BS,max}$ are minimum and maximum BS capacity respectively in (kWh), $P_{BS,ch,max}$ is the maximum charging power of the BS in (kW), and $P_{BS,dc,max}$ is the maximum discharging power in (kW).

Similarly, the following formulas characterised the performance of HS tools. Equation (23) specifies the maximum capacity of the HS tank for each time interval. Additionally, the tank's capacity must be constrained within predetermined minimum and maximum thresholds, as outlined in equation (28).

$$A_{HS}(t) = A_{HS}(t-1) \cdot \varphi_{dsp} + (H_{out} - H_{in}) \quad (23)$$

$$A_{HS} \leq A_{HS,max} \quad (24)$$

Where A_{HS} is HS units, and φ_{dsp} is the dissipation rate of hydrogen which is assumed 0.006 for one year [95].

3.7 Objective function

The PtH system's objective is to maximise income gain during its operating lifespan. The total profits are revenues that come from selling produced hydrogen and surplus electricity provided by renewable sources. In addition, expenditures including the use of the electrical grid, operation and maintenance cost of components, and carbon taxes are considered. The assumption is made that the surplus electricity is sold to the power market in Finland at hourly spot prices.

$$R_{H2}(t) = V_{H2}(t) \cdot C_{H2}(t) \quad (25)$$

$$R_{RES}(t) = P_{RES}(t) \cdot Price_{Gr}(t) \quad (26)$$

$$R_{FC}(t) = P_{FC,el}(t) \cdot Price_{Gr}(t) \quad (27)$$

$$EX(t) = P_{Gr}(t) \cdot Price_{Gr}(t) + OPEX_{AE,fix}(t) + OPEX_{FC,fix}(t) + OPEX_{BS,fix}(t) + OPEX_{HS,fix}(t) + OPEX_{PV,fix}(t) + OPEX_{w,fix}(t) + OPEX_{PV,var}(t) \cdot P_{PV}(t) + OPEX_{w,var}(t) \cdot P_w(t) + Tax_{Gr}(t) \cdot P_{Gr}(t) + Tax_{RES}(t) \cdot P_{RES}(t) \quad (28)$$

Where V_{H2} is the volume of hydrogen in (kg), C_{H2} is the price of hydrogen, P_{RES} is the power of the RE in (kW), $Price_{Gr}$ is grid price, $P_{FC,el}$ is the output power of the FC in (kW), EX is expenditures, OPEX is operating expenditures in ($€/kW$), and (fix and var) index mean fixed and variable.

Furthermore, it is noticeable that the price of producing green hydrogen in recent years is between 4 to 12 $\$/kg_{H2}$ which is reported by IEA [98].

$$OBJ = Profits_{max} = \sum_{t=1}^{T} R_{H2}(t) + R_{RES}(t) + R_{FC}(t) - EX(t) \quad (29)$$

3.7.1 Net present value

Net present value (NPV) is a financial metric that quantifies the difference between the current value of cash inflows and outflows over the whole lifespan of the PtH system. It represents the present value of an upcoming sequence of payments.

$$NPV = - CAPEX + \sum_{y=1}^{N} \frac{Profit(y)}{(1+i)^y} \quad (30)$$

Where CAPEX is the capital expenditures, *N* is the number of years, *y* is the year, and *i* is the interest rate which is assumed a constant amount of 3% for all computational participants.

In the formula, CAPEX appears with a negative sign because it represents the initial outflow of cash required for the investment. This outflow is subtracted from the present value of the cash inflows to arrive at the NPV.

Additionally, the annuity factor (ANF) is used to adjust investment expenditures to account for the effect of interest rates [99].

$$ANF = \frac{i \times (1+i)^n}{(1+i)^n - 1} \tag{31}$$

Where *i* is the interest rate and *n* is the lifetime of the component. The ANF should be applied to all CAPEX values to accurately determine the annual capital investment required for each element. By multiplying the ANF with each CAPEX amount, we can obtain the precise yearly investment needed for all components involved.

3.7.2 Levelized cost of energy

The LCOE in (*€/kWh*) is a metric used to measure the financial expenditure associated with hydrogen generation in terms of energy. It includes both the initial capital outlay and continuous operating expenses.

$$\text{LCOE} = \frac{CAPEX + \sum_{y=1}^{N} \frac{EX(y)}{(1+i)^y}}{\sum_{y=1}^{N} \frac{V_{H2}(y) \cdot LHV_{H2}}{(1+i)^y}} \tag{32}$$

Where LHV_{H2} is the lower heating value of hydrogen which is 33.3 (kWh/kg_{H2}).

3.7.3 Levelized cost of hydrogen

The LCOH in (*€/kg*) signifies the mean net current cost associated with hydrogen creation from a PtH structure concluding its operational period. This metric can be defined using the subsequent formula:

$$\text{LCOH} = \frac{CAPEX + \sum_{y=1}^{N} \frac{EX(y)}{(1+i)^y}}{\sum_{y=1}^{N} \frac{V_{H2}(y)}{(1+i)^y}} \tag{33}$$

3.7.4 Ecological track

The hydrogen carbon footprint ($\varepsilon_{H2}\ in\ kg_{co2,e}/kg_{H2}$) represents the amount of CO2 equivalent ($CO2_e$) emissions per kilogram of hydrogen generated.

$$\varepsilon_{H2} = \frac{\sum_{t=1}^{T}(P_{Gr,b}(t)\cdot\Delta t\cdot\varepsilon_{Gr}\cdot 10^{-3})}{\sum_{t=1}^{T}(H_{AE,out}(t)\cdot\Delta t\cdot LHV_{H2}^{-1})} \quad (34)$$

Where ε_{Gr} is electricity carbon intensity in ($g_{co2,e}/kWh$), which means how many grams of $CO2_e$ is emitted per (kWh) electricity abandoned from the grid. Δt is the duration of the time step in (hr) [85].

4 Case study

In this section, three scenarios are developed using the GAMS software. The software aims to create an optimal model for hydrogen production components. Throughout all simulation stages, the software designs the electrolyser, FC, and hydrogen tank storage capacity to meet demand requirements effectively. Also, other information such as ambient temperature, solar irradiance, and wind speed for the Kannus region in Finland has been collected from the Finnish Meteorological Institute [100] for the year 2023. However, due to the large volume of data, it cannot be included in this document.

Additionally, the surplus electricity is intended to be sold to the grid to generate additional revenue for stakeholders. The software is programmed to determine the best price at which to sell this surplus electricity, utilizing hourly electricity price data for the year 2023 which is gathered from ENTSO-E [101] to inform its decision-making process.

Furthermore, the software is tasked with maximizing the total income generated by the system. This involves employing mathematical equations outlined in the previous chapter to calculate revenue from various sources and optimizing the system configuration to achieve the highest possible revenue output and hydrogen production.

The specified scenarios are defined as follows:

- Scenario 1: In this situation actual data of solar PV and wind parks with a total capacity of 150 MW and 45MW respectively is considered. In this scenario, there is no limitation on the budget and investment.
- Scenario 2: this setup evaluates some limitations in the initial funds and investment. As a result of less budget the capacity of renewable power sources and other components were decreased.
- The third scenario's condition is the same as the second scenario plus reducing the capacity of the BS to diminish capital investment more and increase the electrolyser capacity to produce more hydrogen.

All scenarios will be explained in detail in the next chapter and the price of hydrogen is assumed to be 6.5 €/kg constant in each scenario.

4.1 Input data

This section includes most of the data appropriate to the power to hydrogen system, which involves various data sets related to processes and technologies for converting electricity into hydrogen gas.

Table 4 illustrates the data related to the solar PV plant in the Kannus region in Finland. The plant's rated AC power and peak DC power are 151.8 MW and 168.1 MW respectively. The type of panel structure is the one-axis tracker.

Table 4. Solar PV characteristics

Solar PV	**Value**	**Unit**	**Ref**
Plant rated power	151,8	kW_p	3Flash Finland Company
PV panel area	2.75	m^2	
Number of PV modules	266,825		
Nominal modules efficiency ($\eta_{PV,ref}$)	22.5	%	
Temperature coefficient (α)	-0.300	%/°C	
NOCT	45±2	°C	
Test condition temperature (T_{ref})	25	°C	
CAPEX	650	€/kW	[85]
Fixed OPEX	13.22	€/kW,y	[102]
Variable OPEX	1×10^{-3}	€/kW,y	[7]
Lifetime	20	year	[5]

Table 4 demonstrates wind farm characteristics in which the model of the turbines is V162 IEC S made by Vestas Company for the Kannus wind farm. The rated power of a turbine is 6200 kw with a hub height of 150 m. Also, the standard operating temperature range is from -20°C to +45°C.

Table 5. Wind turbines characteristics

Wind Turbines	**Value**	**Unit**	**Ref**
Cut-in wind speed	3	m/s	[103]
Cut-out wind speed	25	m/s	[103]
Total plant rated power	45,000	kW	[103]
Hub height (h)	149	m	[103]
Hub height wind speed	7.52	m/s	[104]
CAPEX	1,450	€/kW	[105]
Fixed OPEX	20	€/kW,y	[7]
Variable OPEX	8×10^{-3}	€/kW,y	[7]
Lifetime	20	year	[5]

Table 6. Electrical characteristics

Characteristics	**Value**	**Unit**	**Ref**
Electricity consumption tax*	0.63	€/MWh	[106]
VAT	24	%	[106]
CO2 tax	53	€/ton	[106]
Renewable tax**	0.01	€/MWh	
Grid tax***	0.78	€/MWh	
Interest rate	3	%	
Project lifetime	30	year	
Electricity GHG intensity in 2022	66	$gCO2_e$/kWh	[107]
Carbon footprint of renewable hydrogen	3 ~ 4	kg_{CO2e}/kg_{H2}	[108]

* The electricity consumption tax class 2 is defined by the Finnish Energy Agency and Tax Office Authority, which includes companies, manufacturing, and industry sectors.

** In this study, the assumption of negligible CO2 emissions from renewable sources allows for the incorporation of renewable taxes into the calculation of the objective function.

*** The grid tax encompasses the electricity consumption tax for class 2 along with the value-added tax (VAT).

Furthermore, the research operates under the assumption of a fixed interest rate, and it is presumed that the value of the Dollar ($) is equivalent to that of the Euro (€).

Table 7. Alkaline electrolyser characteristics

AE	Value	Unit	Ref
Minimum power	5% of rated power		[109]
Maximum power	100% of rated power		[109]
Efficiency	63 ~ 71	%	[110]
CAPEX	1,700	€/kW	[98]
OPEX (annual)	4% of CAPEX	€/kW	[111]
Lifetime of the stack	10	year	[112]

Table 8. PEM Fuel cell characteristics

PEMFC	Value	Unit	Ref
Maximum power	100% of rated power		
Efficiency	45	%	[113]
CAPEX	1250 ~ 5000	€/kW	[113]
OPEX (annual)	4% of CAPEX	€/kW	[114]
Lifetime	40	hr	[113]

In Tables 7 and 8, characteristics of AE and PEMFC are presented. Across all scenarios, the rated power of both electrolyser and FC varies. However, in all scenarios, the software aims to design the appropriate components to achieve an optimal system in the second and third scenarios, the rated power capacity of these two elements was adjusted downwards by implementing a constraint in hydrogen sales to reduce investment costs.

Table 9. Battery and hydrogen storage characteristics

BS & HS	Value	Unit	Ref
Battery storage (Li-ion)			
Charging efficiency	95	%	[115]
Discharging efficiency	95	%	[115]
State of charge range	20 ~ 100	%	[115]
Minimum power	0		[116]
Maximum power	5,000	kW	[116]
Minimum energy	0		[116]
Maximum energy	20,000	kWh	[116]
CAPEX	306	€/kWh	[117]
OPEX (annual)	2% of CAPEX	€/kW	[115]
Lifetime of the module	10	year	[115]
Hydrogen storage			
CAPEX	500	€/kg	[118]
OPEX (annual)	2% of CAPEX	€/kg	[119]
Maximum allowable pressure	350	bar	[120]
Lifetime	30	year	

5 Simulation results and discussion

This chapter provides a comprehensive explanation of all the scenarios simulated by the software, detailing the results obtained to illustrate the process of the power to hydrogen system. The objective is to identify the most efficient methods to maximize both hydrogen production and revenues. Additionally, it is important to note that some values are significantly high due to the substantial power input from wind and solar PV sources, which consequently leads to the accumulation of large numerical values. This segment will delve into these aspects, offering insights into the scale and impact of using extensive RESs in the hydrogen production process.

To begin with, each scenario is described sequentially from 1 to 3. Following these descriptions, a sensitivity analysis is conducted to assess the impact of hydrogen price variations on the objective function and the net present value. This analysis aims to provide a deeper understanding of how fluctuations in hydrogen pricing can influence the overall economic feasibility and effectiveness of the power to hydrogen system. By examining these factors, the study seeks to identify the optimal conditions and strategies for maximizing profitability and efficiency in hydrogen production.

Furthermore, to streamline the process given the extensive input data, certain modifications have been made. For instance, instead of using hourly electricity prices for all 8760 hours in a year, an average price for each hour of a day in a month has been calculated. This results in 24 average values per month. This method has been applied consistently for all input data over the 12 months of the year. Ultimately, each month is represented by one day with 24 hourly values, summing up to a total of 12 days.

5.1 Scenario I

In this section, it is assumed that there are no budgetary or investment limitations, allowing the use of the actual value of the power sources. This part is divided into two models: one without constraints and one with a constraint on hydrogen sales.

The first case introduces a constraint on hydrogen sales, limiting them to 200 tonnes. This constraint is imposed to manage the size of the electrolyser, accommodate the trade of surplus electricity to the grid, and account for uncertainties in hydrogen demand. In the second case, all power generated from renewable sources and the grid is converted into hydrogen gas and there is no surplus electricity for selling.

Both cases are evaluated using the software to determine the most effective strategy. The first model insights into the implications of limiting hydrogen sales and optimizing the system under real-world market conditions, while the second model provides the potential to maximize hydrogen production without any selling constraints. The analysis of these scenarios aims to identify the optimal balance between hydrogen production, system efficiency, and economic returns.

5.1.1 Case 1

This section examines a constraint maximum selling of 200 tonnes of hydrogen to meet the demand. Due to uncertainties on the demand side and the unpredictability of how much hydrogen can actually be sold, this limit is maintained. Additionally, considering the presence of large power plants in the region, enforcing this limit provides the option to sell surplus electricity to the grid. This excess electricity could potentially support a significant number of household or industrial needs. Implementing this strategy not only helps in managing the demand fluctuations for hydrogen but also promotes the sustainability of the system by ensuring that extra energy is efficiently utilized, thereby supporting the overall energy infrastructure, and reducing waste.

Given the substantial amount of output data generated for each month, only the months of January, March, June, September, and December have been selected as representative samples. This approach avoids the need to present all the results and charts for every month, making the analysis more manageable and focused. By choosing these specific months, which cover different seasons and operational conditions, we can still capture the variability and key trends in the data without overwhelming the presentation with excessive information.

The electrolyser size, FC size, and hydrogen tank are intended to be designed for all scenarios. In this case, their values are 10 MW, 0, and 180 kg respectively. The FC size has been excluded from all scenarios because the software's analysis determined that incorporating it would be financially unsuitable. The affordability constraints identified by the software indicate that integrating FC is improper, making it an impractical option within the given budgetary limits. As a result, the design strategically omits the FC to maintain economic viability. Additionally, the software calculated the financial values of LCOE, LCOH, CI, and objective function (OBJ) which are 0.077 €/kW, 2.555 €/kg. 0.149 g_{CO2}/kWh, and 360 million euros (M€) respectively.

The power balance figures for case 1 are as follows:

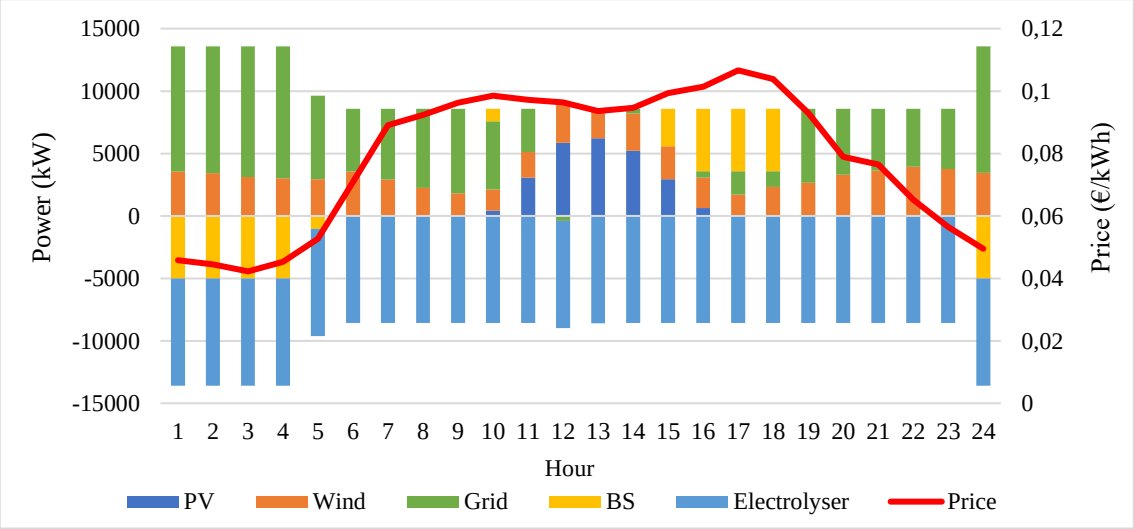

Figure 13. Power balance for January

Figure 13 shows the power balance for the month of January, incorporating data on solar PV power, wind power, grid power, BS, power used by electrolyser, and Finland electricity prices. Due to the reduced sunlight in January in the region, the PV power makes a minimal contribution during the daylight. In contrast, wind power significantly participates almost all day, peaking around midday. The grid frequently supports the system to compensate for the shortfall in renewable power. Meanwhile, the BS charges during the early hours of the day when electricity prices are low. This stored energy is then used in the afternoon when electricity prices are at their peak.

The power used by the electrolyser shows a relatively constant consumption throughout the day, with minor variations. This constant demand suggests that the electrolyser operation is not significantly influenced by the diurnal patterns of renewable energy generation.

The analysis of the power balance for January indicates a significant contribution of RESs during daylight hours, which helps reduce the grid's dependency and stabilises electricity prices. However, the reliance on grid power remains high during early morning and evening.

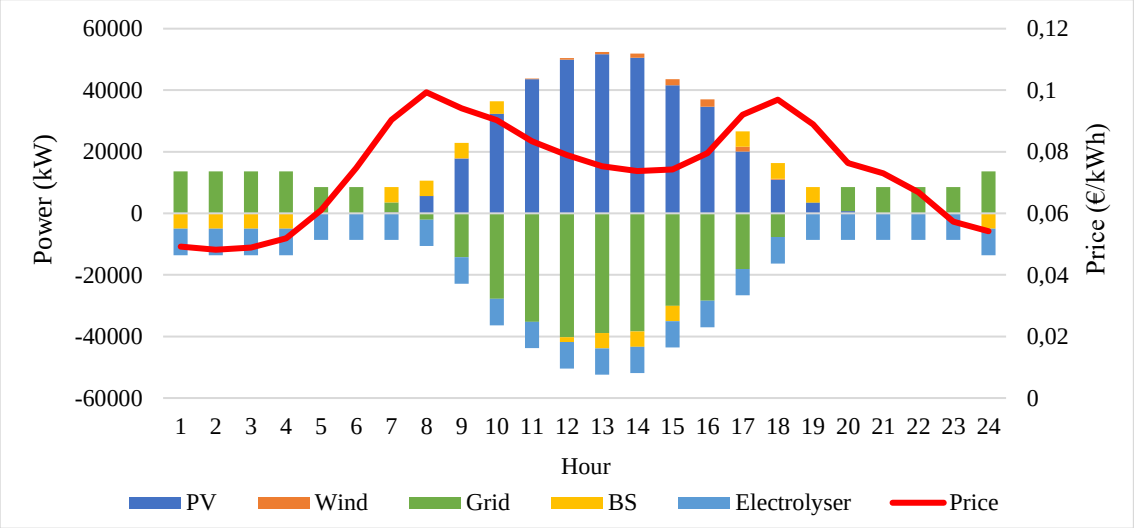

Figure 14. Power balance for March

Figure 14 point out the power balance for the month of March. PV power shows an excessive contribution during midday hours. As a result of insufficient wind speed during this month, wind power has not significantly supported the system, except for a minor involvement throughout the day, with a notable peak around the afternoon. The grid power supplements the system during periods of low renewable energy generation. It shows a role during the early morning and evening hours when the price of electricity is low, reflecting higher demand and lower renewable output during these times.

During this month surplus renewable and stored electricity is sold to the grid, which is represented as negative values on the chart during these hours. Also, the BS is utilised to support the electrolyser's operation. Although the electrolyser may not be functioning at full capacity during these peak times, the system is optimally designed to produce hydrogen consistently throughout the month.

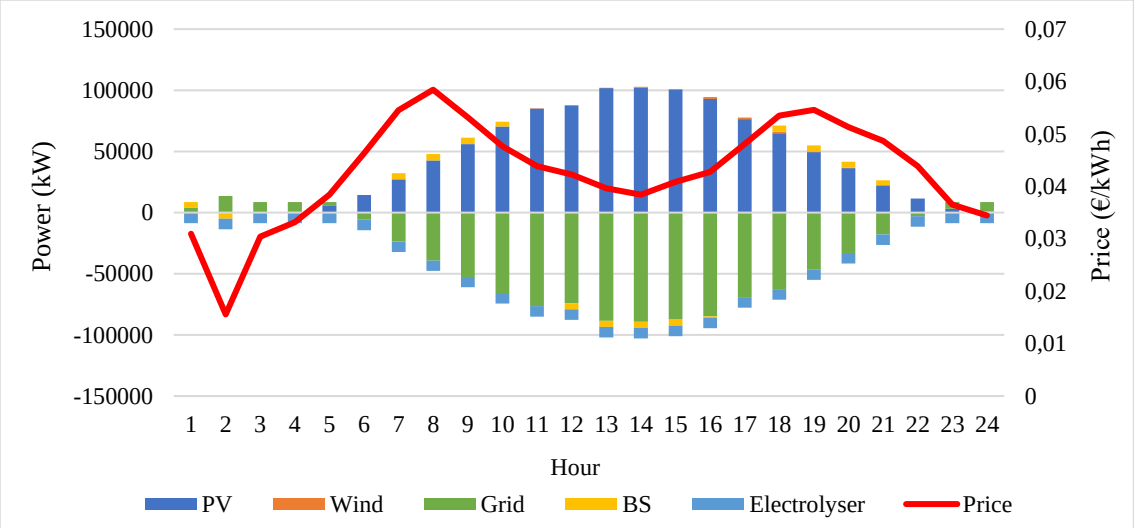

Figure 15. Power balance for June

In June, PV power shows a considerable provision during daylight hours, peaking around noontime. This is indicative of the longer daylight hours and higher solar intensity during the summer months. On the other hand, wind power impact is low throughout the day, with minor peaks that complement solar generation.

As displayed in the figure, grid usage is at its lowest level among all the selected times due to the high availability of renewable power sources, particularly solar PV. In addition, the BS are charged occasionally and discharged during the morning and evening. Furthermore, the period for selling surplus electricity has been expanded according to having lots of solar energy, resulting in higher revenue for stakeholders this month. It should be noted that the electrolyser operates regularly and steadily at its minimum capacity for hydrogen production and the focus of the system is selling extra electricity.

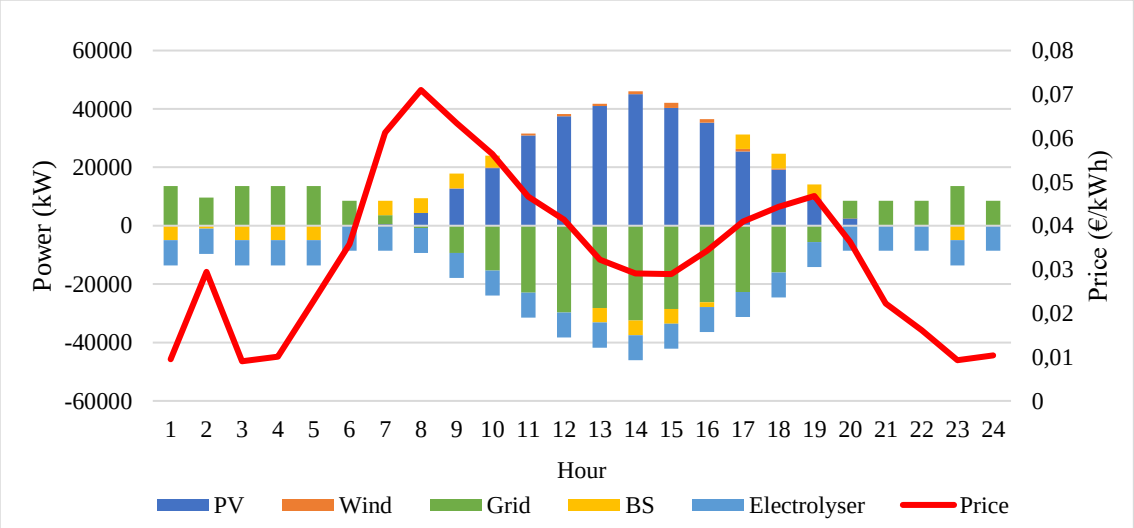

Figure 16. Power balance for September

Based on the Figure 16, the power balance in September operates in a relatively stable manner, ensuring consistent hydrogen production, electricity sell, and BS usage. During this month, PV power is utilised more extensively than wind power due to favourable weather conditions.

Compared to June, in September, the electricity prices are at their lowest during the early morning hours from 2 to 6 AM and from 8 to 11 PM. During these periods, the grid is utilised to support the operation of the electrolyser. As well, the BS charges when prices are low to offset the renewable power deficit and ensure the stable operation of the electrolyser. Besides, it discharges and supplies power when electricity prices are high, continuing until the prices gradually decrease. This leads to effectively balancing supply and demand. Conversely, surplus electricity is sold to the grid, with the maximum additional power around midday. Despite fluctuations in energy production, the electrolyser operates without fail to ensure continuous hydrogen creation.

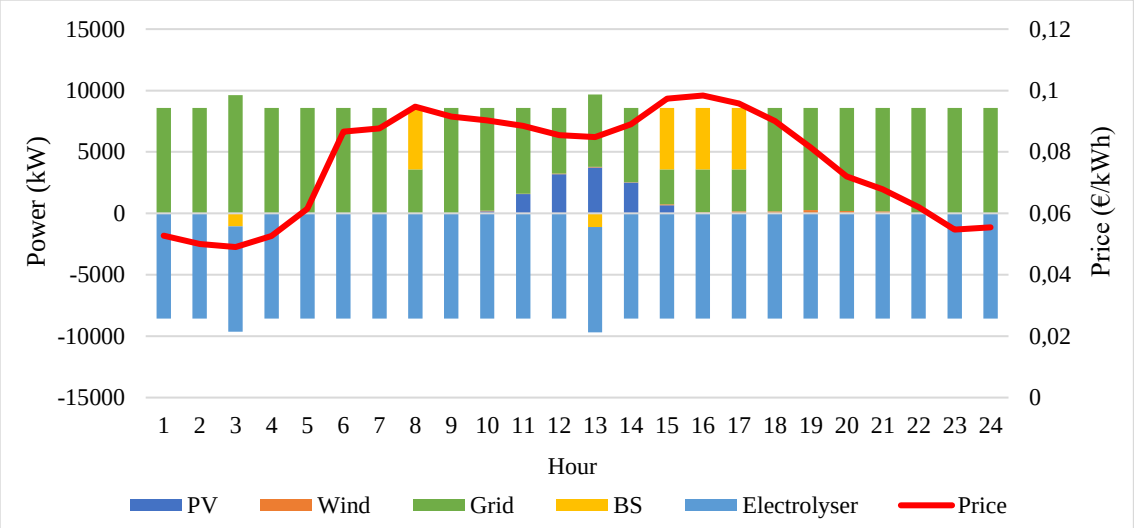

Figure 17. Power balance for December

Figure 17 presents the power balance for December. In this month PV power generation is minimal because of shorter daylight hours and lower solar intensity. The impact of PV power is almost negligible throughout the day, which is expected during winter months in Finland.

Despite the expectation of higher wind speeds in the winter, wind power, like solar PV, remains negligible and is at its lowest level during all the aforementioned month. Grid power plays a crucial role in December, particularly during times when RESs are insufficient. The usage of grid power peaks throughout the day, highlighting a heavy reliance on grid energy to compensate for the shortfall in renewable power sources.

It can be seen that BS is used to strengthen the system. It charges during periods of low electricity prices and discharges during peak price periods. This strategy helps balance the power supply and manage costs effectively. The power balance for December shows a meaningful dependence on grid power due to the lower availability of PV and wind power. Despite there is not enough renewable power, the electrolyser functions every time based on support by the grid, ensuring permanent hydrogen making.

In addition to the power balance analysis, the specific characteristics of each component were thoroughly examined. All components were analysed across the five selected months to demonstrate their behaviour at different hours of the day. This comprehensive analysis provides insights into how each component performs under varying conditions throughout

the year. By evaluating their performance during these different months, we can understand the operational dynamics and efficiency of each component in response to seasonal changes.

- Battery SOC

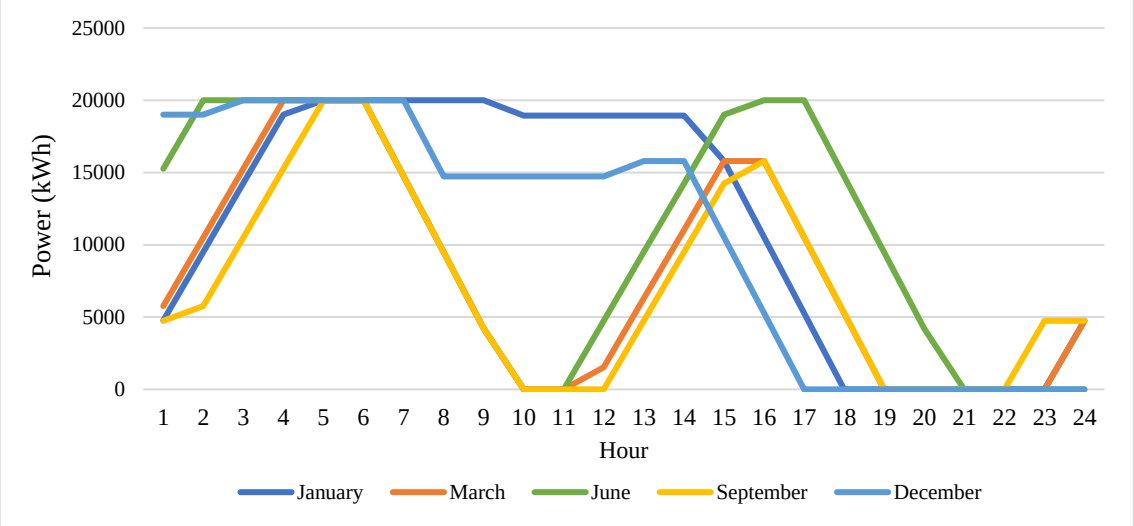

Figure 18. Battery storage characteristics

The graph illustrates the BS state over 24 hours in the declared date. In January and December, the BS charges significantly, peaking at 20 MWh, and remains fully charged during the day, likely due to lower electricity prices and sufficient grid or renewable energy. March and September show a similar charging and discharging pattern with a notable fluctuation, representing normal use of batteries by supply and demand. June's sample exhibits a wide workload compared to the other months because of the availability of solar PV, higher daytime demand, and lower grid availability.

The system's ability to charge during low-cost periods and discharge during high-demand times ensures cost-effectiveness and reliability. Seasonal variations dictate the extent and timing of battery usage, underscoring the need for adaptable energy management strategies to optimize performance and maintain grid permanency throughout the year.

- Solar PV power

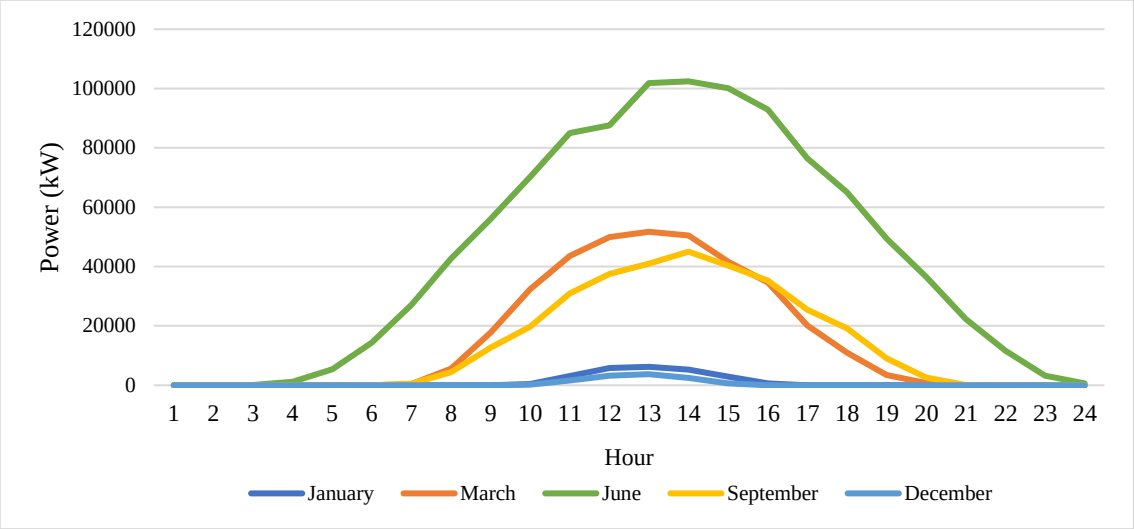

Figure 19. Solar PV characteristics

The solar PV output varies significantly with the seasons. Summer month, June, provides optimal conditions for the highest output due to longer daylight hours and maximum solar intensity, while winter months, January and December, show the lowest output due to shorter days and lower solar intensity.

- Wind turbines power

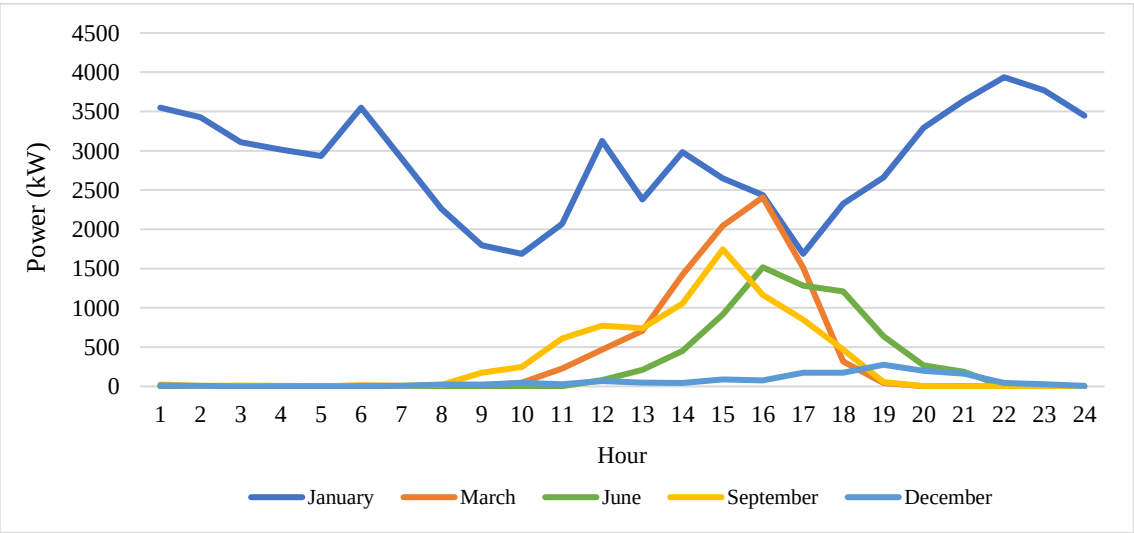

Figure 20. Wind turbines characteristics

Figure 20 indicates that January stands out as the most productive month for wind power, providing constant and high energy output. In contrast, December presents challenges with significantly lower wind power generation. March, June, and September outline the average power generation peaks in the afternoon with little differences in the time.

- Grid power

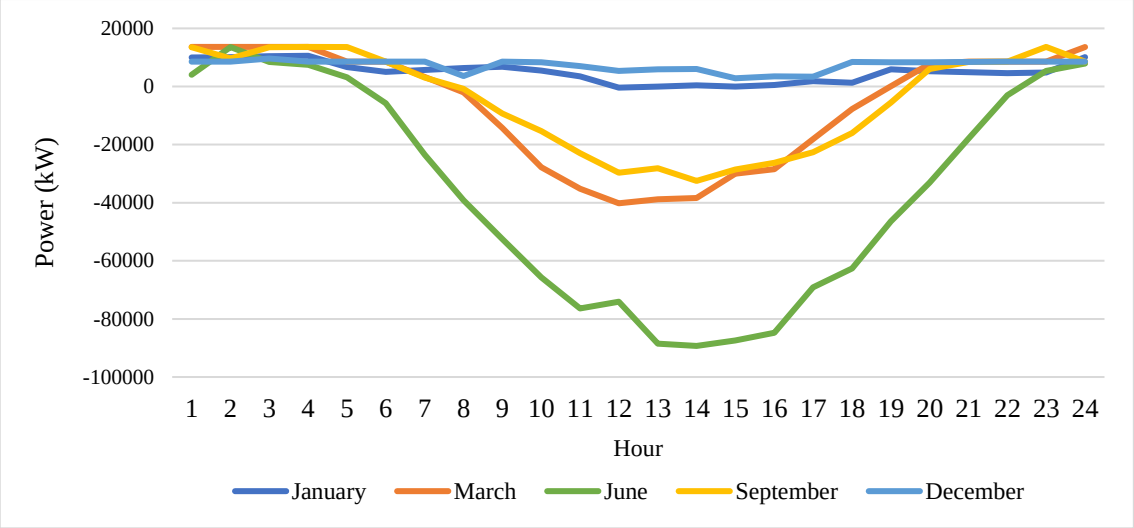

Figure 21. Grid characteristics

The analysis of grid power utilization over five months underlines the dynamic interplay between the grid and RESs. The substantial dips into negative values during midday in the summer months reflect the high impact of solar PV generation, significantly reducing grid dependency. In other words, the negative side means there is an income by selling additional electricity. Winter months show a more stable reliance on grid power due to lower renewable energy contributions.

Across all months, there is a general shape of declining grid power usage in the morning, reaching a low point around noon and recovering in the evening. This form aligns with the availability of solar power, wind power, and BS which reduces the need for grid power during daylight hours.

- Battery charging

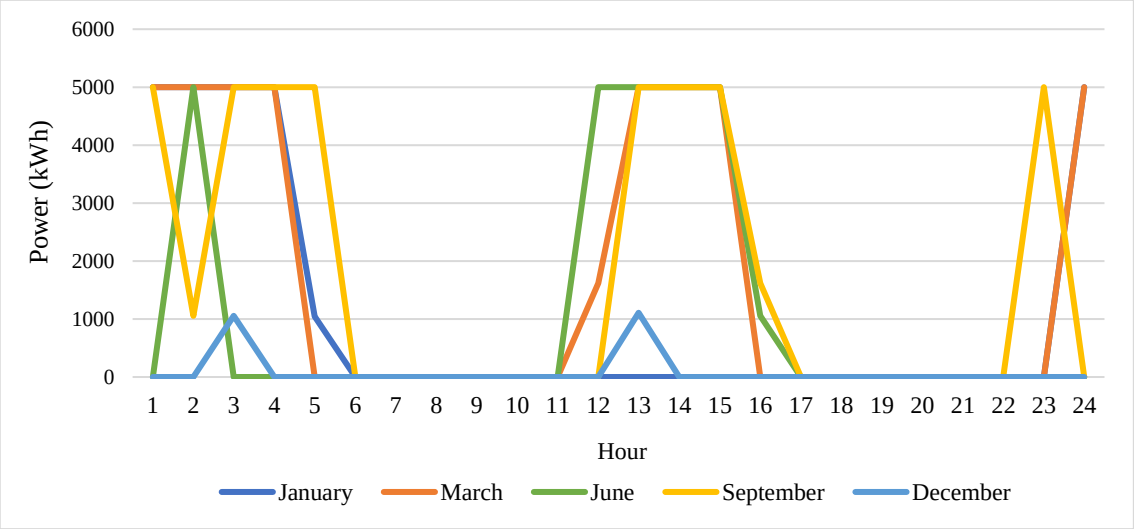

Figure 22. Battery charging characteristics

The analysis of battery charging samples highlights the strategic use of off-peak hours for charging to optimize cost savings and ensure energy availability during peak demand periods. Seasonal variations significantly impact the charging patterns, with summer months benefiting from high solar PV output allowing for additional midday charging, while winter months face challenges with reduced renewable energy availability.

September exhibits a distinct charging repetition with significant charging periods in the early morning, midday, and late evening leveraging high energy output.

In contrast, in December, the charging form is less pronounced compared to other months. This reduced charging activity reflects the lower availability of solar PV and wind power during the winter months, necessitating a more conservative charging strategy to ensure energy availability.

- Battery discharging

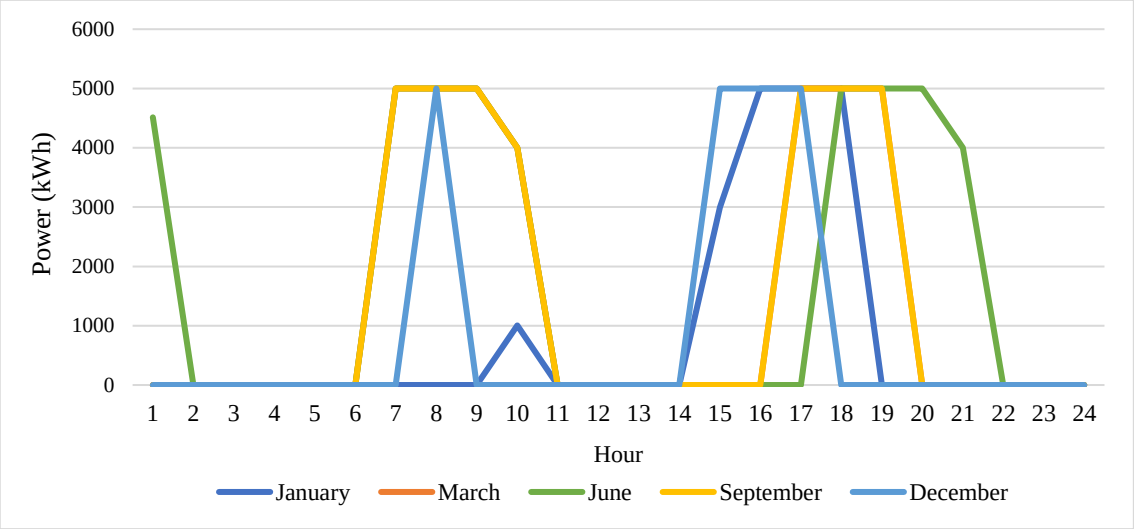

Figure 23. Battery discharging characteristics

As it is shown in Figure 23, in winter months like January and December, the BS discharges primarily in the morning and afternoon to compensate for reduced solar and wind power availability. This emphasizes the importance of having robust energy storage to meet higher demand during periods of low renewable energy generation. Conversely, summer months such as June benefit from higher solar output, resulting in extra midday discharging sessions.

March and September graphs are the same and show intermediate examples, with the BS discharging during both morning and afternoon peaks, reflecting transitional periods with rational renewable energy availability and demand. December presents encounters with concentrated discharging sessions in the morning and afternoon, reflecting the difficulties in meeting energy demands with reduced solar and wind power availability.

The discharging peaks steadily reach around 5000 kWh particularly in the afternoon until night in all months, demonstrating the battery system's ability to provide substantial supplemental power during high demand periods.

5.1.2 Case 2

This section validates the simulation results under optimal conditions without constraints. The software, leveraging electricity price data, determines that hydrogen production is more cost-effective than selling electricity to the grid. As a result, there is no revenue generated from selling renewable power. This strategic decision leads to significantly high values in key financial metrics, including CAPEX, NPV, and OBJ. The high CAPEX indicates substantial initial investments in infrastructure and technology. The elevated NPV reflects strong long-term profitability, while the optimized OBJ features the efficiency and effectiveness of the overall system design in maximizing economic returns. These outcomes demonstrate the financial viability and potential benefits of prioritizing hydrogen production over direct electricity trade.

In case 1, the power balance was analysed over a span of five months, which serves as the foundational framework for all scenarios considered. To streamline the presentation and avoid an overload of data and figures, we will focus on two representative months, January and June, in this part of the analysis. These months have been selected to provide a clear and concise illustration of the power balance dynamics under varying seasonal conditions. January represents the winter period with its unique challenges and energy patterns, while June exemplifies the summer period with distinct solar power contributions.

In this case, the electrolyser size is 200 MW, and the hydrogen tank capacity is 400 kg. Additionally, the software's calculations have yielded several key economic and environmental metrics such as LCOE, LCOH, CI, and OBJ which are 0.016 €/kWh, 0.533 €/kg, 0.094 g_{CO2}/kWh, and 4860 M€ respectively.

Furthermore, the power balance figures are illustrated as follows, providing detailed visual representations of the energy flow and distribution within the system.

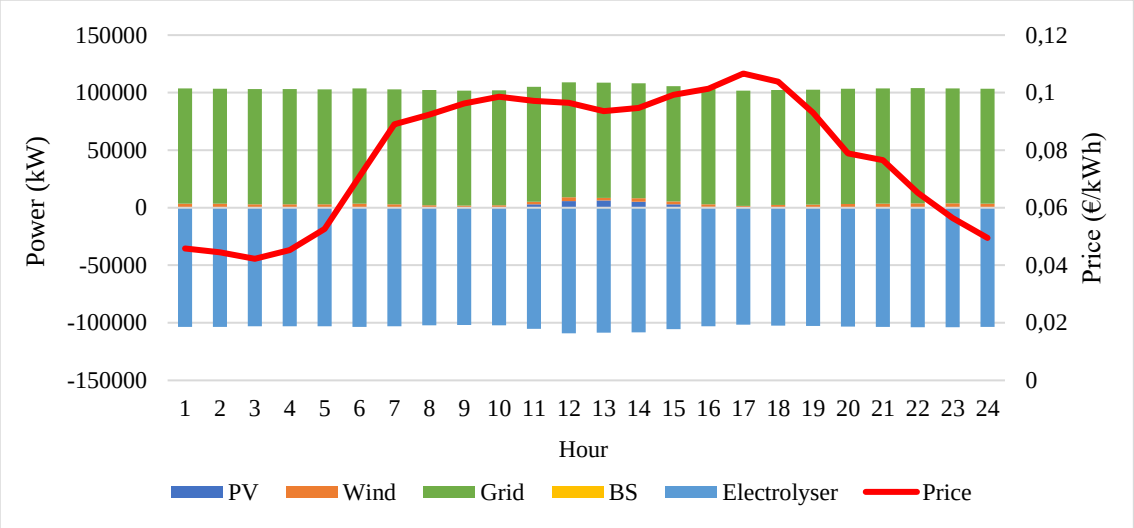

Figure 24. Power balance for January

Figure 24 depicts a power balance graph for the month of January. The absence of significant PV and wind power generation indicates that January is a month with low renewable energy output. This could be due to seasonal variations affecting solar insolation and wind patterns. Obviously, with low renewable generation, the system relies heavily on grid supply without taking into account the price of electricity. As a result of high price of electricity, there is no availability of BS in this month and the software prefers to use the grid directly and convert it to hydrogen. The electrolyser appears to be operating at full capacity without any pauses.

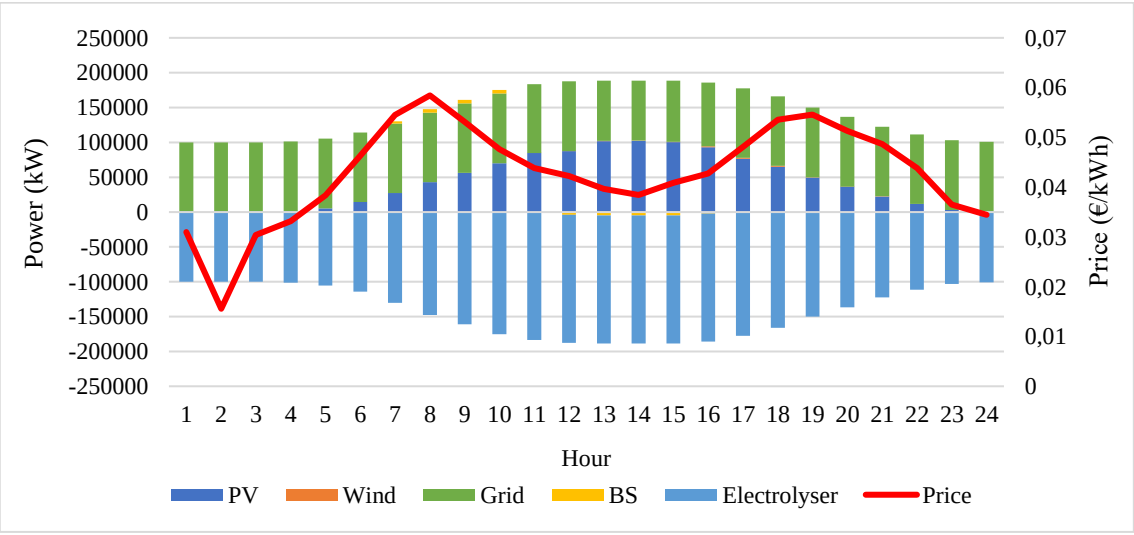

Figure 25. Power balance for June

Figure 25 illustrates the power balance of June. The electricity price is the same as the last power balance for this month. However, unlike the constrained scenario, this chart demonstrates much more operation of the electrolyser and unavailability of surplus electricity for selling. The limited utilisation of the BS suggests that the system prioritises direct consumption of renewable and grid power, possibly due to the lower costs and sufficient generation capacity. During the day particularly in the midday the use of solar PV is significant, this results in reduced dependency on the grid during daylight hours. On the other hand, wind power is still in low operation. The reliance on the grid fluctuates with higher dependence during off-peak PV hours, highlighting the role of the grid in balancing supply.

In addition, the hydrogen balance for these two months is as follows:

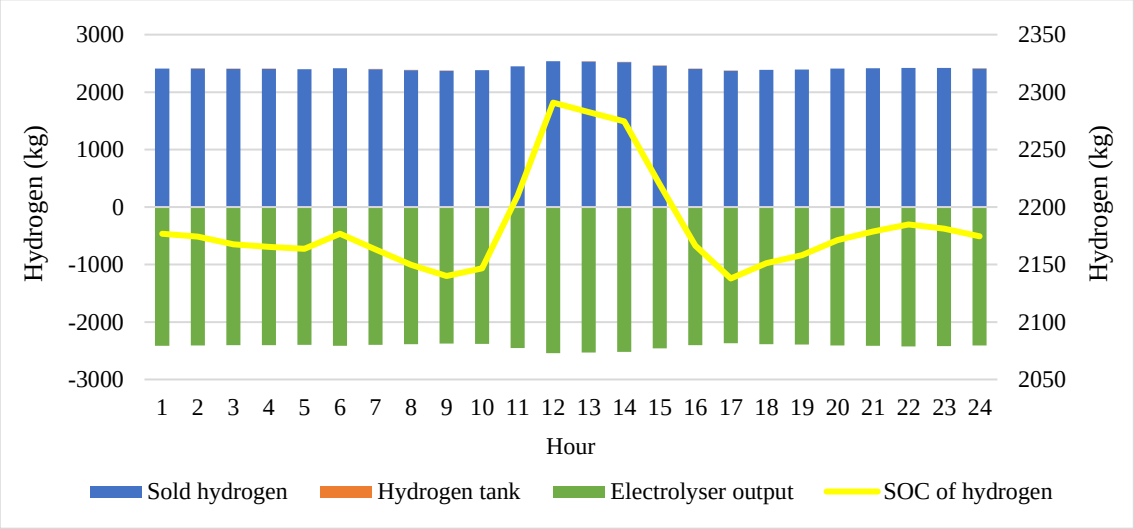

Figure 26. Hydrogen balance for January

Figure 26 implies the hydrogen balance graph for January with stable and well-managed hydrogen production. There is a consistent balance between demand and production. The significant peak in the state of charge around midday, as shown by the yellow line, could be attributed to increased production or decreased consumption of hydrogen during this time. The midday peak in the state of charge suggests opportunities for optimization in production and storage management. Additionally, the state of the hydrogen tank indicates that there is generally only a small amount of hydrogen stored during daytime and around midnight.

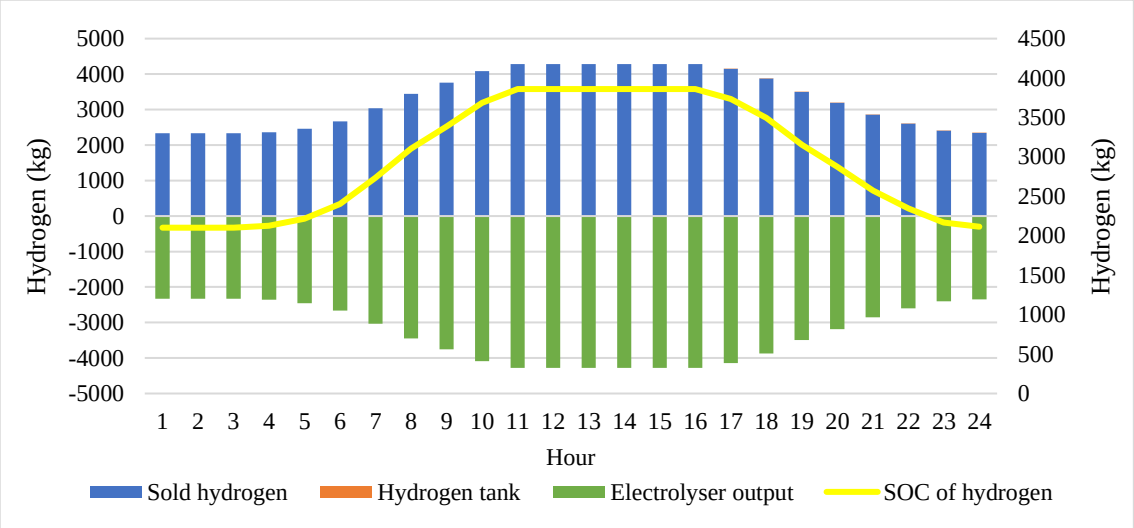

Figure 27. Hydrogen balance for June

Figure 27 displays a system that effectively leverages high renewable energy availability to optimize hydrogen production and sell. Strong hydrogen trade, with a peak during the middle of the day, suggests that hydrogen creation is aligned with high solar energy availability. The significant peak in the state of charge around midday implies that hydrogen production exceeds consumption during these hours, leading to an increase in storage levels. As illustrated, the storage tank quantities are low from the afternoon until midnight, and prior to that, all produced hydrogen is sold. Moreover, other figures for the case 2 are as follows:

- Battery SOC

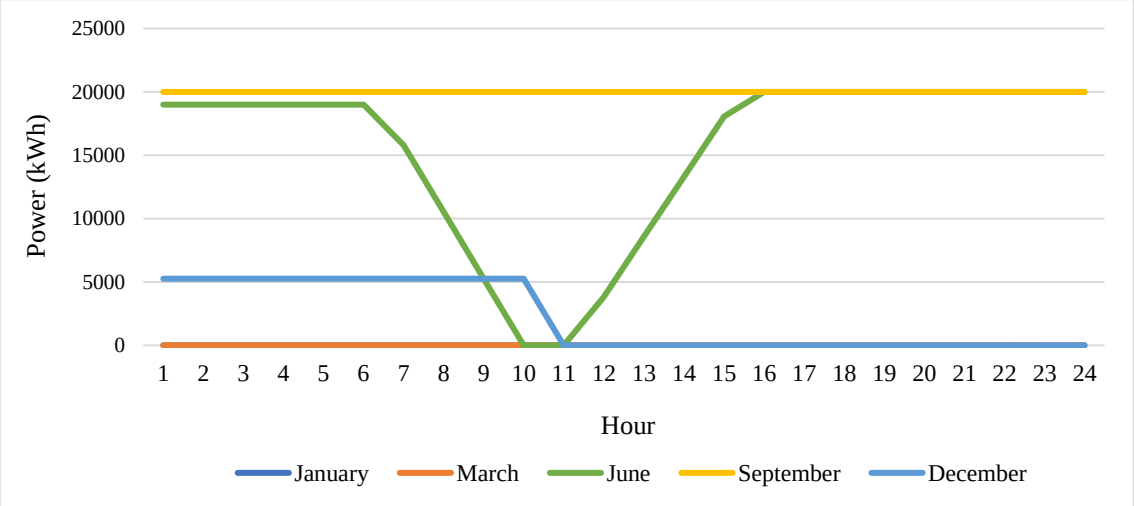

Figure 28. Battery SOC characteristics

The SOC graph in Figure 28 shows distinct seasonal patterns. January and March are the absence of any charging and discharging due to lack of renewable power or the high price of electricity. In December, the SOC is at the minimum level in the morning and then drops around noon, after that, it has been discharged fully. June displays a dynamic arrangement with charging in the early morning, discharging from 7 AM to 11 AM, and recharging in the afternoon, reflecting high solar energy convenience. September maintains a high SOC throughout the day, indicating ample renewable energy, grid support, and low consumption of the battery. These variations highlight differing energy management strategies and renewable energy availability across the months.

- Grid power

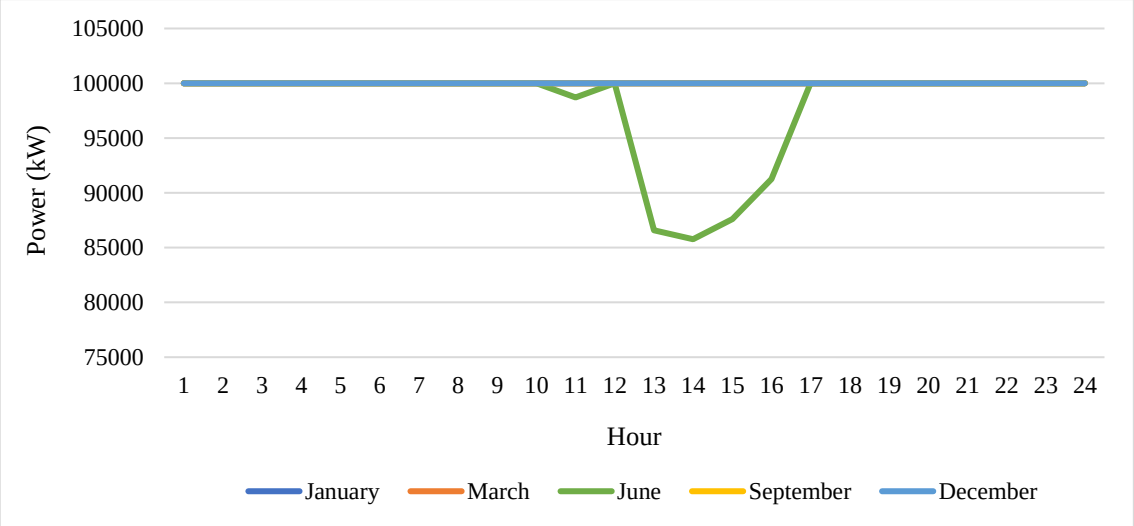

Figure 29. Grid characteristics

Figure 30 depicts the grid power workload. The key point is the impact of solar PV in June, which influences grid performance. During midday to early evening in June, most power for the electrolyser comes from PV. At other times, the grid serves as the primary supplement to the system at its highest adjusted level.

- Input power of electrolyser

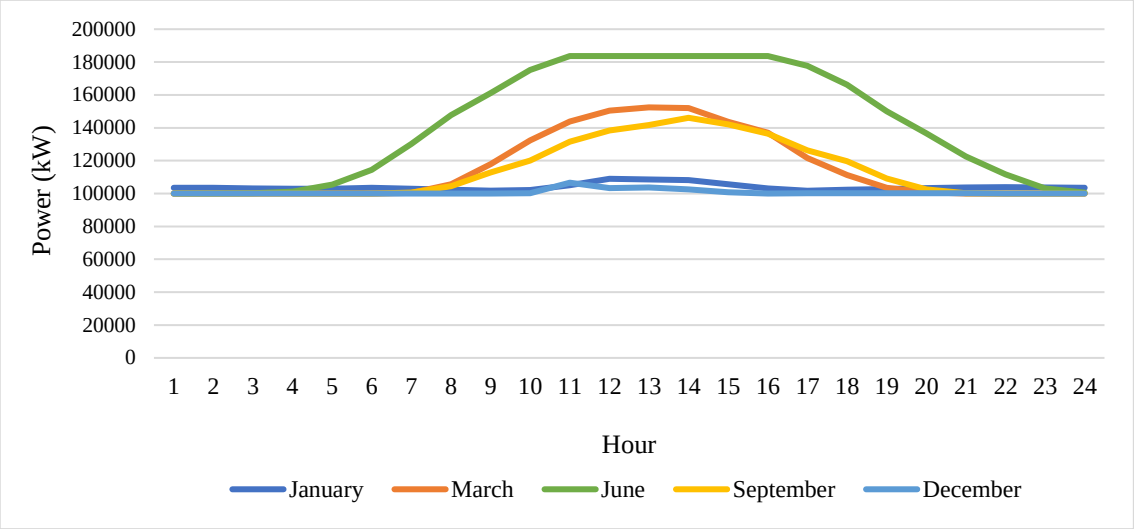

Figure 30. Electrolyser characteristics

Figure 30 point out the electrolyser's operation under various conditions. In June, March, and September the electrolyser operates at regular capacity, benefiting from abundant solar energy plus grid. Conversely, in January and December, the electrolyser operates at a minimal level due to limited renewable power, yet it maintains stability to produce hydrogen as a result of supporting totally by the grid. In this section, the electrolyser runs without any constraint of generating hydrogen accordingly consumes much power. Likewise, this model shows that it needs to have a large capacity of electrolyser.

5.2 Scenario II

In the second scenario in order to decrease the budget and investment the capacity of all components was diminished. Consequently, each renewable power source has a capacity of 15 MW, the maximum BS capacity decreased to 10 MWh, and the grid capacity is 50 MW, which is half of the previous scenario. The electrolyser and storage capacities were designed by the software. Additionally, there is a constraint of 70 tonnes for hydrogen trade. This adjustment optimizes system performance to better reflect a real business environment. The analysed and designed values of electrolyser and hydrogen tank dimensions for the second

scenario are 3.5 MW and 63 kg in turn. Furthermore, economic quantities for LCOE, LCOH, CI, and OBJ are 0.048 €/kWh, 1.596 €/kg, 0.252 g_{CO2}/kWh, and 126 M€ respectively.

The power balance statistics are as follows:

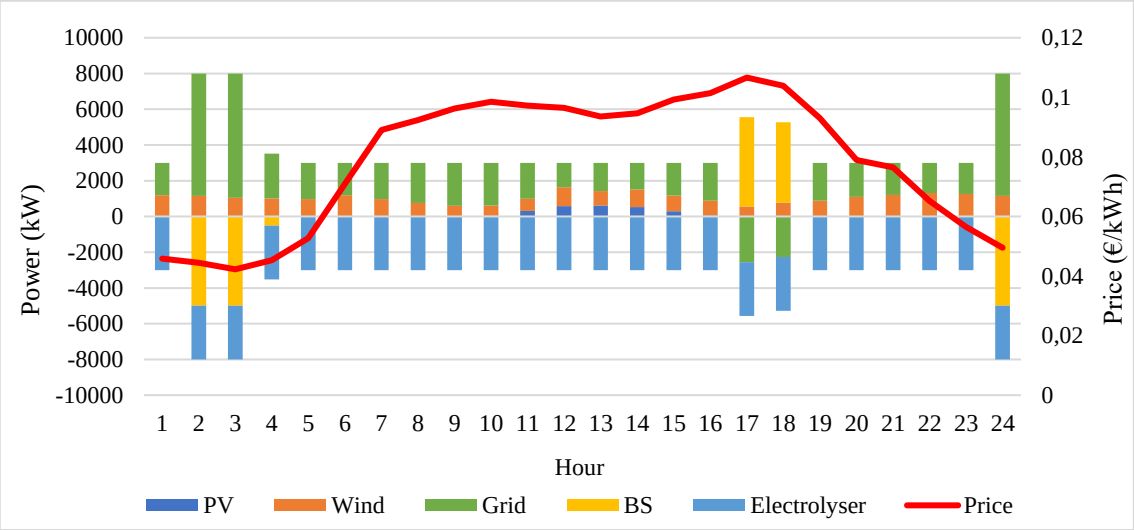

Figure 31. Power balance for January

As shown in Figure 31, the PV represents minimal generation during midday and shows its low role as a result of short daylight. Wind power provides a steady though modest contribution throughout the day which can support the electrolyser. Grid power usage remains relatively stable, highlighting its position as a reliable power source and supplement. The BS, with noticeable activity in the early morning and late evening, indicates periods of charging due to the low price of power and discharging at the high price of electricity, directing selling further electricity. The electrolyser is primarily driven by the grid with the availability of renewable energy and supported by BS during peak price periods. This balance showcases a strategic use of available power sources to optimize cost and efficiency.

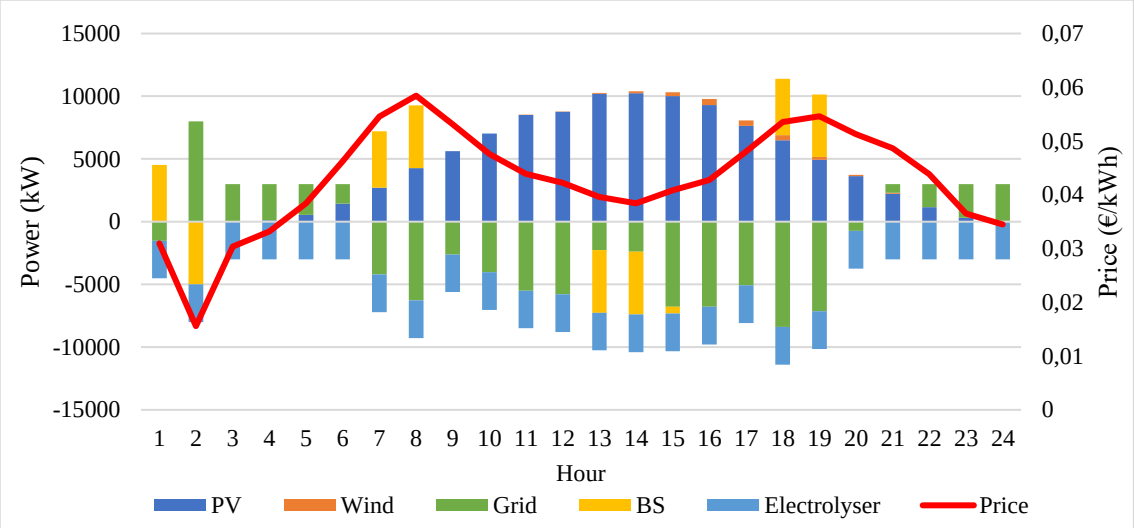

Figure 32. Power balance for June

Figure 32 illustrates the power balance for June, depicting a PV generation peaks significantly from the morning to early night. This considers high solar obtainability during these hours. Wind energy provides a little bit of power throughout the afternoon. Grid power is used almost less, and peaks in the early morning due to the low price of electricity. It is still used around midnight when solar power is not available. The BS shows charging and discharging patterns that complement the PV generation. With notable discharges in the morning and late evening at a high price of power, try to support the system. The electrolyser aligns with the availability of solar power, indicating optimal use of renewable energy for hydrogen production. This power balance highlights efficient energy management, leveraging high solar generation in June to minimize grid dependency and optimize electrolyser operation. Furthermore, as it can be seen there is more excess electricity at a negative level which makes a significant revenue for stakeholders.

In the following, other components characteristics will be analysed:

The characteristics of the two renewable sources, solar PV and wind, are the same as the previous scenario. The primary difference lies in the magnitude of power generation, which has decreased due to the reduced capacity of these sources.

- Grid power

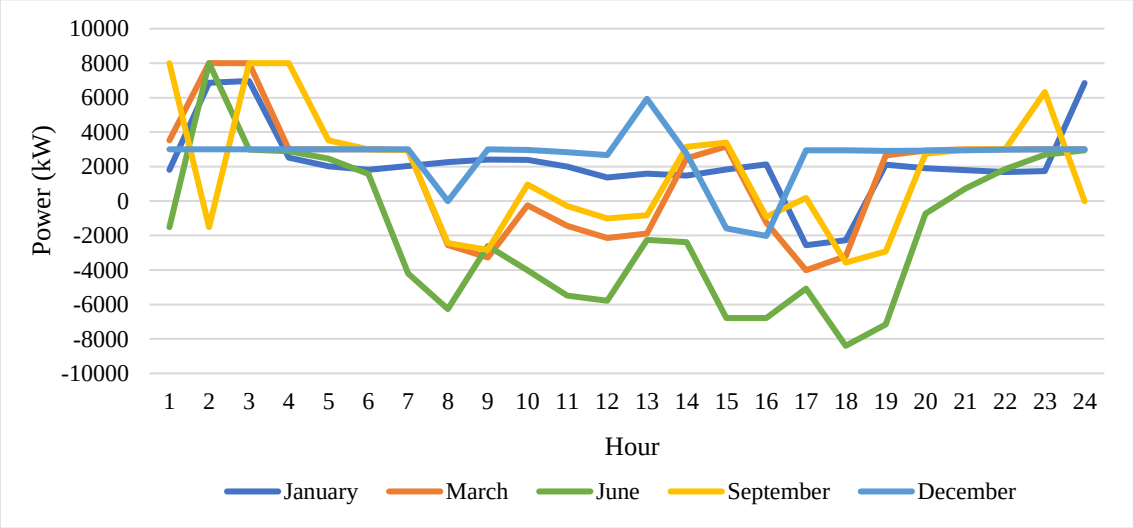

Figure 33. Grid characteristics

Figure 33 shows grid power generation across the mentioned months. In March, September and particularly June there is disposal of extra electricity as a result of more renewable power. This leads to a significant income for the investors. On the other hand, in December and January, grid power is stable with slight peaks and fluctuations in the early morning and late night. Besides, less use of power generation by the grid happened in January due to having suitable wind power. This highlights the grid's role in balancing power supply based on the availability of RESs.

- Battery charging

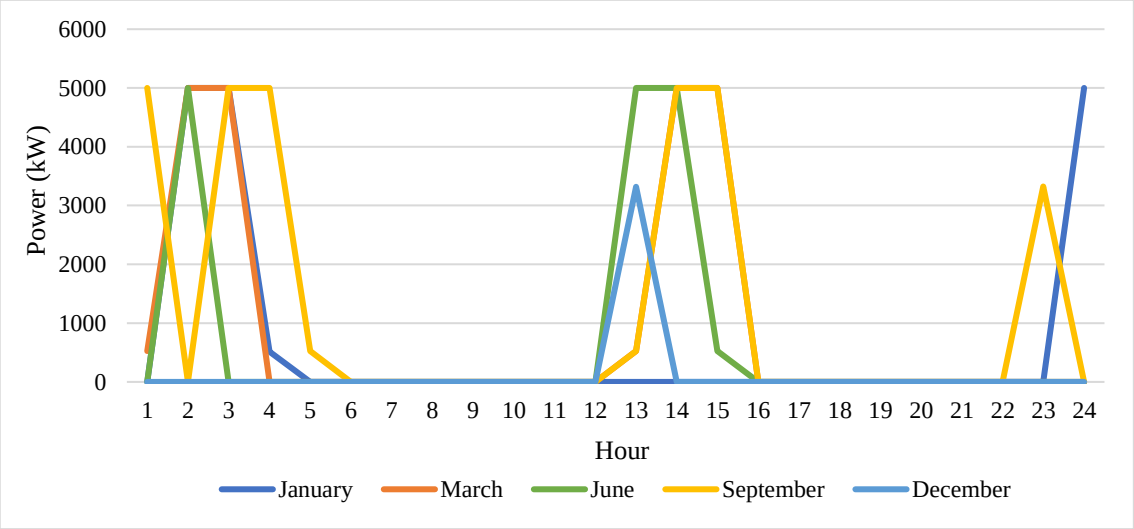

Figure 34. Battery charging characteristics

The graphs of Figure 34 points to the battery charging characteristics for the stated months. Charging activity is concentrated during specific hours for each month. In January in the early morning because of having proper wind power, it charges to use for the rest of the day. The most limited charging occurred in December due to a lack of insufficient renewable energy accessibility and higher grid dependency. The most variation happened in September as a result of having enough green sources of energy. In March and June charging peaks, corresponding with higher solar generation. These two months' graphs almost are the same.

- Battery discharging

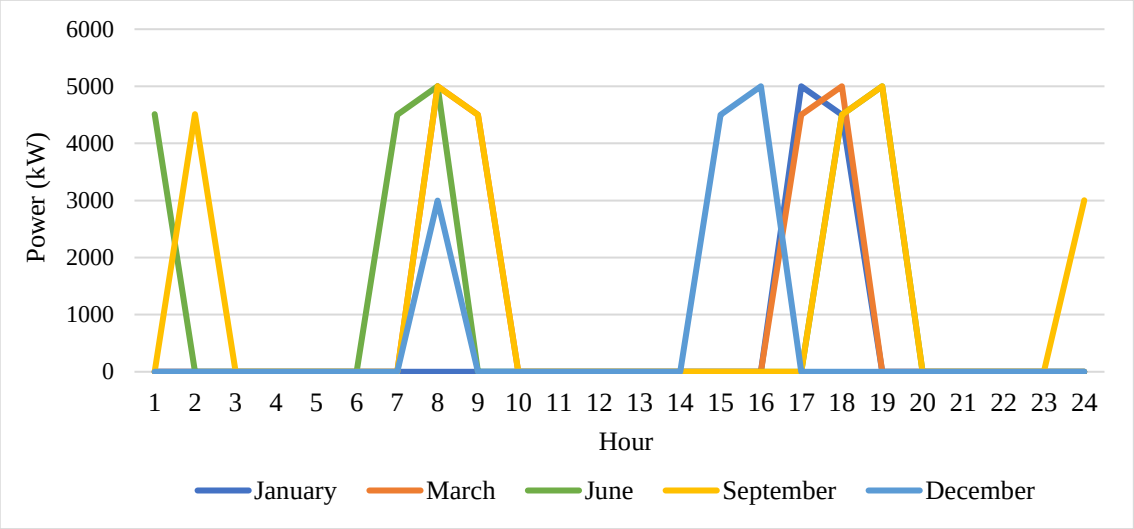

Figure 35. battery discharging characteristics

This figure indicates that battery usage peaks in the morning and evening for all months. In January, batteries have been deactivated throughout the day except in the evening due to scarce renewable power and grid support. March, June, and September exhibit the most oscillations, benefiting from adequate RESs. Consequently, stored energy in the batteries has been discharged to support the electrolyser, with any excess sold back to the grid.

5.3 Scenario III

This scenario mirrors the second scenario but differs in the capacities of the batteries and the electrolyser. To minimize investment in BS, the maximum capacity has been reduced to 5 MW. Conversely, the capacity of the electrolyser has been increased by raising the hydrogen sell constraint to 100 tonnes. This adjustment aims to balance the system by relying less on BS and more on direct hydrogen production, contemplating a strategic shift towards maximizing electrolyser utilization and enhancing hydrogen output. The suggested electrolyser and hydrogen tank volumes are 5 MW and 90 kg in scenario 3. The other financial results of LCOE, LCOH, CI, and OBJ are 0.034 €/kwh, 1.140 €/kg, 0.204 g_{CO2}/kWh, and almost 170 M€ respectively.

The power balance of scenario III is as follows:

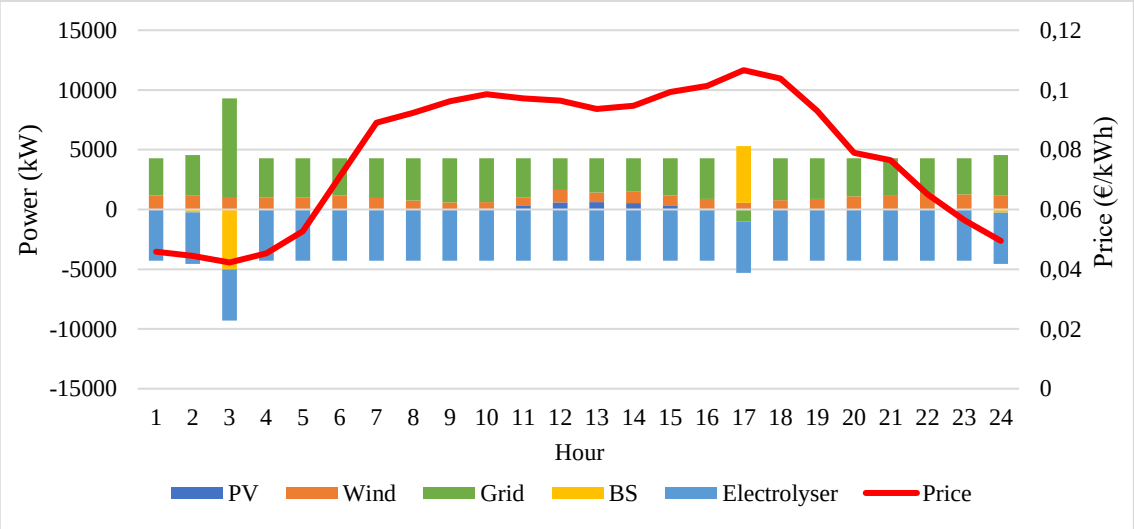

Figure 36. Power balance for January

As indicated in Figure 36, the usage of batteries in this scenario is less due to reducing the capacity of that. In the lowest price of electricity, in the early morning battery is charged for further utilisation. Also, solar PV has had a negligible effect as a result of the shortfall in sunlight. However, wind power influences the system during this month, but the system relies on the grid significantly. Electrolyser operation is normal with the proper workload.

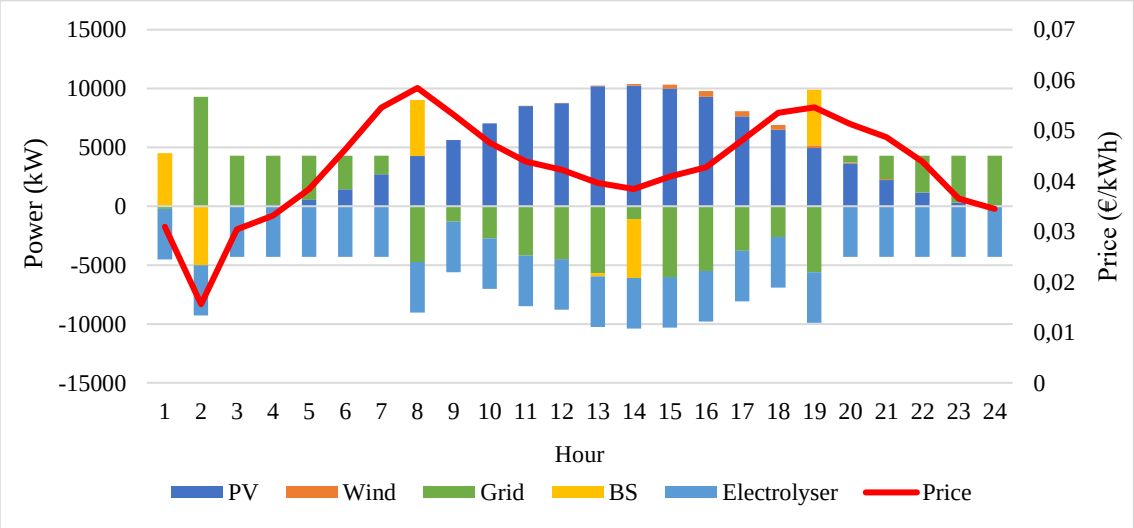

Figure 37. Power balance for June

Figure 37 shows the suitable situation for batteries and solar PV. Due to having proper and long daylight, batteries were charged and when the price was at the highest level, discharged to assist the system. In addition, solar PV has its maximum level of operation during the day. On the other hand, as the wind speed is not appropriate, the undertaking of wind turbines is less. Except in the early morning, in the other times of the day not only utilisation of the grid is smaller amount but also there is excess electricity for selling to the grid.

For comparison and realising the condition of changes, only grid and BS circumstances are explained. The state of the other components is almost similar to the second scenario.

- Grid power

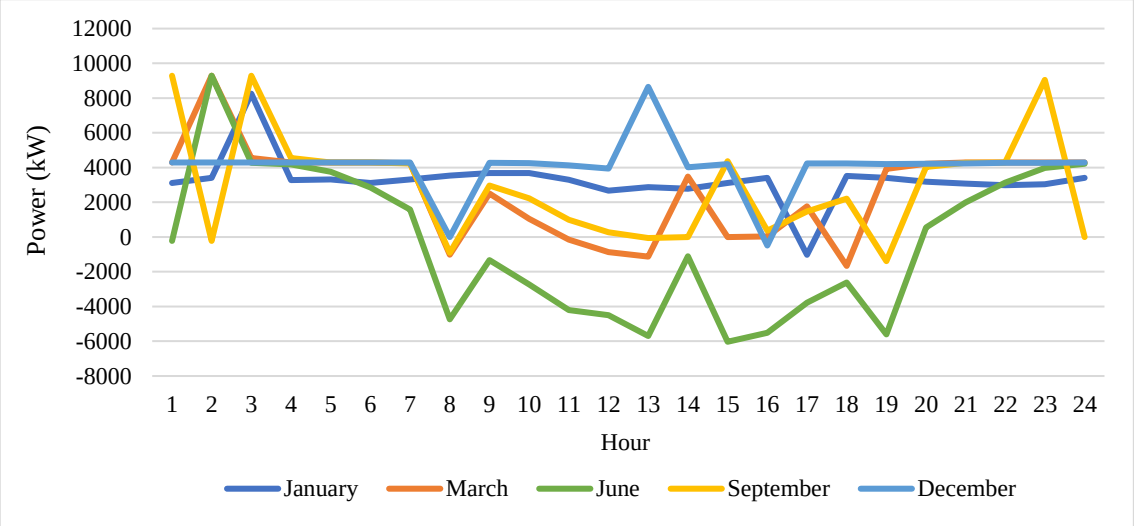

Figure 38. Grid power characteristics

As can be seen in the Figure 38, There are significant fluctuations in power generation and consumption by the grid. For instance, June stands out as the most profitable month for sponsors like the previous scenarios. Conversely, the power generated in March and September, while not conducive to profit-making, is well suited for supporting the electrolyser in hydrogen production. In contrast, the electricity generated in January and December has a uniform effect on the system and does not yield profits.

- Battery charging

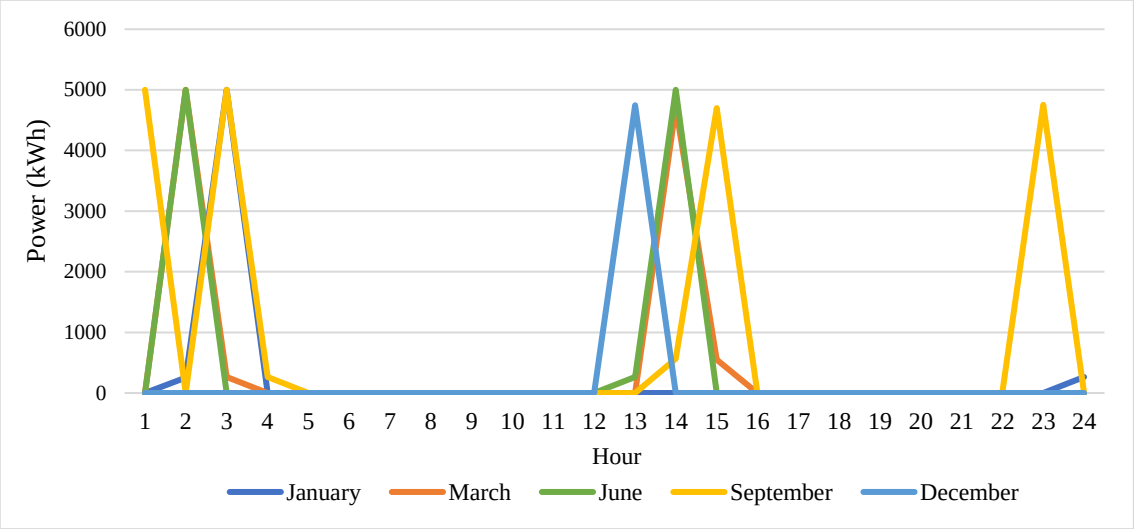

Figure 39. Battery charging characteristics

This figure depicts the battery charging status. January and December exhibit almost identical conditions, differing only in charging times. Both months frequently showed low charge levels, in the early morning and around the afternoon, due to limited solar PV availability. In March and June, battery conditions are similar due to the use of solar power. The power balance graph indicates a significant workload for the batteries in these two months. September, however, shows greater fluctuations in battery charging due to the combined accessibility of solar and wind power. Since the figure illustrates, charging time mostly happened in the early morning and afternoon for all mentioned months.

- Battery discharging

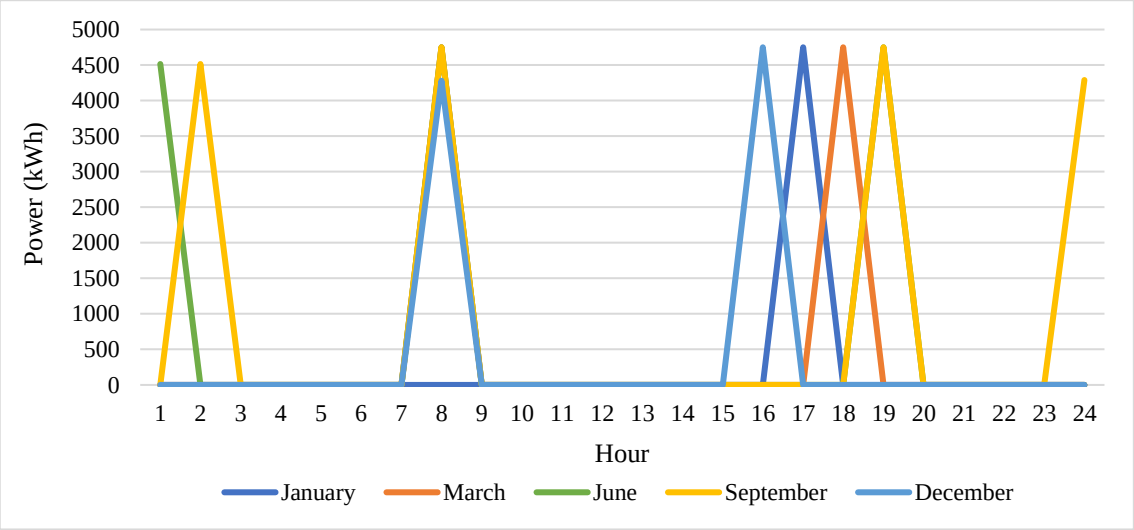

Figure 40. Battery discharging characteristics

Figure 40 shows the battery discharging model for the revealed months. Due to the disposal of renewable electricity in March, June, and September, batteries were charged. Consequently, as clarified by the figure the most discharging occurred in the late afternoon till early night in those months. It is noticeable that within this time frame batteries are fully discharged to reach their minimum level of energy storage to uphold the system in the peak time of electricity usage. January demonstrates a weak process compared to the above-mentioned periods since the stored energy in the batteries is insufficient. Batteries have a normal discharging activity in the morning and early afternoon in December as well.

5.4 Economic outcomes of the scenarios

The economic outcomes of the three scenarios and two sub-models outlined in the table below demonstrate considerable variations influenced by different constraints and operational parameters. This analysis, conducted using specialised software, aims to determine which model offers superior performance and generates greater revenue for investors. By examining key metrics such as CAPEX, NPV, LCOE, LCOH, and OBJ the software provides a detailed comparison, highlighting the financial implications and

potential returns associated with each scenario. This comprehensive evaluation is crucial for stakeholders to identify the most economically viable option and make informed investment decisions in the hydrogen production and storage sector.

Table 10. Economic characteristics

	Sc 1				
	Case 1	**Case 2**	**Sc 2**	**Sc 3**	**Unit**
Hydrogen tank	180	400	63	90	Kg
Electrolyser size	10	200	3.5	5	MW
Maximum $H_{2,sell}$	200	4,280	70	100	tonne
CAPEX	12,500	267,554	4,375	6,250	k€/kW
$CAPEX_{tot}$	139,404	394,458	30,493	31,063	k€/kW
NPV	335,583	4,446,846	117,881	168,639	k€/year
OBJ	358,525	4,855,833	125,923	180,135	k€/year
LCOE	0.077	0.016	0.048	0.034	€/kWh
LCOH	2.555	0.533	1.596	1.140	€/kg
Carbon Intensity	0.149	0.094	0.252	0.204	g_{CO2}/kWh

In this table $CAPEX_{tot}$ represents capital expenditure of all components including solar PV, wind turbine and BS. It should be noted that for the objective function, only CAPEX was taken into account, with the assumption that RESs and batteries were already established. For calculating the LCOE and LCOH, $CAPEX_{tot}$ was considered.

5.5 Sensitive analysis

This section describes a scenario involving adjustments in price and economic consequences. Specifically, the price of hourly electricity is fixed at 0.2 €/kWh. All other parameters and variables are fixed with those in the first scenario, which includes restrictions on hydrogen sales. In this scenario, the software assesses the impact of these conditions on the net present value and the objective function. The evaluation provides visions into how maintaining a constant electricity price influences the overall economic performance and financial viability of the system.

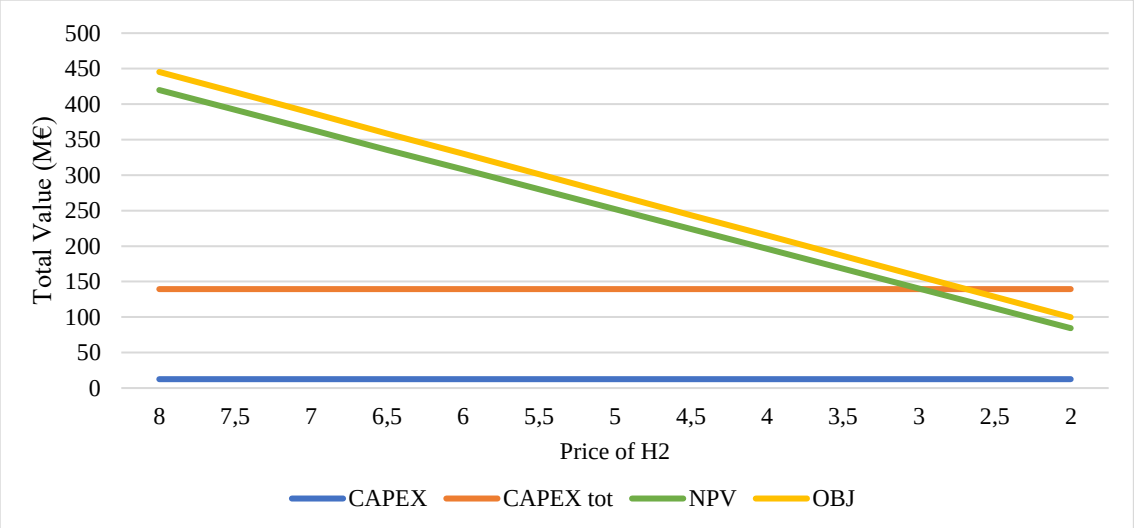

Figure 41. Sensitive assessment

The chart illustrates that the price of hydrogen sold is not static, undergoing stepwise reductions by half a euro. As the price of hydrogen declines, the income correspondingly diminishes. This trend stresses the direct relationship between the price of hydrogen and the resulting income, emphasizing that lower hydrogen prices lead to lower revenue levels. The stepwise pattern of the price reduction is depicted in the chart, demonstrating a systematic approach to analysing the impact of price changes on revenue.

5.6 Discussion

This section discusses the operational dynamics of the model. As illustrated in Figure 12, the system is designed to utilize the FC to convert surplus hydrogen into electricity when demand for hydrogen is low or non-existent. This excess electricity is then sold to the grid. However, during the simulation, the software opted not to use the FC, instead directly transferring the remaining electricity to the grid to maximize immediate profit.

While this approach effectively reduces total expenditure, it also presents certain advantages and potential opportunities for the system. On one hand, directly selling excess electricity to the grid lowers operational costs and enhances immediate revenue streams. On the other hand, maintaining flexibility in how excess electricity is managed can be highly beneficial. For instance, the system could redirect extra electricity back into the electrolyser when needed, providing a cost-effective means to produce more hydrogen when demand increases.

Additionally, the potential use of FC introduces further benefits. FC can support the establishment of charging stations for electric vehicles (EVs), which can serve as a valuable asset for the infrastructure. This multi-functional use of FC not only diversifies the system's capabilities but also aligns with broader goals of promoting sustainable energy management.

Furthermore, since the specific data pertains to the year 2023, it is important to consider that the results may vary when different input data and conditions are applied. This variability discusses the need for ongoing analysis and consideration of various factors that could influence the outcomes.

Overall, the discussion highlights the trade-offs and strategic decisions involved in managing spare electricity within the model. The ability to balance immediate profit with long-term flexibility and extra functionalities, such as EV charging stations, underlines the importance of a holistic approach to optimizing the system’s performance and economic viability.

6 Conclusions

The conclusion of this thesis provides a comprehensive analysis of a power to hydrogen system, demonstrating various scenarios to identify the most efficient strategies for maximizing hydrogen production and revenue. The simulations via the GAMS software incorporated different limitations and functioning considerations, proposing precious perceptions of the system's performance under diverse circumstances. Three scenarios plus sensitive analysis were simulated and then assessed in the simulation and result sections.

Scenario I explores a model without financial or investment boundaries, focusing on two sub-models: one with a constraint on hydrogen sales and one without any bounds. The first sub-model limits hydrogen sales to 200 tonnes to manage electrolyser size and accommodate surplus electricity trade. The second sub-model maximizes hydrogen production by converting all power to hydrogen.

The analysis indicates that managing hydrogen sales constraints can optimise system efficiency and economic returns by balancing production with market conditions. In case 1, the LCOE and LCOH for the mentioned time are normally equal to 0.077 (€/kWh) and 2.555 (€/kg) respectively. Consequently, compared to the results of the other scientific papers named in this study these values show the validity of these results. Also, the capacity of the electrolyser and hydrogen tank volume is 10 MW and almost 200 kg. Additionally, the amount of CI is negligible equal to 0.149 g_{CO2}/kWh which shows the sustainability issues in this study are preserved. OBJ is roughly 360 M€ shows an extreme amount of profit.

In case 2, which operates without limitations, the values for LCOE, LCOH, and CI are 0.016 €/kWh, 0.533 €/kg, and 0.094 g_{CO2}/kWh respectively. These exceptionally low amounts indicate that large-scale hydrogen production significantly reduces the levelized cost of energy and hydrogen, thereby increasing revenues which is almost 4860 M€. The designed electrolyser and HS size are 200 MW and 400 kg in turn. However, this sub-model has an extremely low value of the levelized cost of energy and hydrogen, it requires substantial investment and may necessitate government support due to the high financial demands. Besides, its feasibility and implementation are at the lowest level of performance.

Scenario II reduces the capacity of all components, reflecting a more realistic business environment. RESs are capped at 15 MW, grid capacity at 50 MW, and BS at 10 MWh, with a 70 tonnes constraint on hydrogen trade. This scenario emphasizes economically effective strategies, highlighting the efficient utilization of renewable energy and grid power to support hydrogen production. As the electrolyser and HS size are 3.5 MW and almost 70 kg respectively, this suggests that a balanced approach with reduced capacity and strategic constraints can maintain profitability while minimizing investment. In this scenario, LCOE, LCOH, CI, and OBJ are 0.048 €/kWh, 1.596 €/kg, 0.252 g_{CO2}/kWh, and 126 M€ respectively which confirms the direct association between hydrogen production and its cost level.

Scenario III further adjusts the capacities, reducing BS to 5 MW and increasing the electrolyser capacity by raising the hydrogen sell constraint to 100 tonnes. This scenario shifts the focus towards maximizing electrolyser size around 5 MW and HS scope near 100 kg. The results show that increasing hydrogen production capacity, while reducing reliance on BS, can enhance economic returns and system performance. In this model, as there was a decrease in battery size the LCOE diminished to 0.034 €/kWh due to less use of batteries. Also, LCOH, CI and OBJ in this scenario compared to the second scenario are a little bit lower equal to 1.140 €/kg, 0.204 g_{CO2}/kWh, and 180 M€ respectively.

The economic outcomes of the three scenarios reveal significant variations influenced by constraints and running issues. Key metrics such as CAPEX, LCOE, LCOH, CI, NPV, and OBJ were analysed to determine the most financially viable model. The analysis underscores the importance of optimizing component capacities and strategic constraints to achieve a balance between investment costs and profitability. Accordingly, based on the gained values scenarios II and III are more feasible and realistic.

Likewise, altering the constraint on hydrogen sales directly impacts the LCOE and the LCOH. For instance, in the first scenario, reducing the constraint of hydrogen sales to 100 tonnes would result in a significant increase in the LCOH, raising it to approximately 5 €/kg. This example illustrates how sensitive the cost metrics are to changes in production and sell limits, emphasizing the importance of optimizing these parameters to achieve commercial efficiency in hydrogen production. Also, Table 10 shows the financial parameters for all scenarios and sub-models.

Sensitivity analysis further illustrates the impact of hydrogen price variations on the objective function and net present value. Nonetheless, the price of electricity in this part remains constant equivalent to 0.2 (€/kWh), the results indicate a direct correlation between hydrogen price and income, highlighting the need for a systematic approach to price management to maximize revenue.

It is important to note that the FC in this model did not operate due to its unaffordability, as determined by the software. Despite numerous attempts have done to activate it, involving extensive adjustments to functionality and various parameters, the FC ultimately remained inactive. Yet, the model did not incorporate the FC effectively, but its economic role has been counted. This outcome stresses the necessity for further research to make FC integration economically viable in future implementations.

Furthermore, several paths for future studies can be proposed to further enhance the understanding and optimisation of this work. Since the FC was excluded from the current model, future research could focus on exploring ways to reduce the costs associated with FC technology. Assessing the long-term benefits of integrating FCs in terms of operational flexibility and grid stability could provide a more holistic view of their value.

Future studies could use advanced optimization algorithms to determine the ideal sizes of system components (electrolyser, HS, RESs, etc.) under different operational constraints and economic conditions.

Moreover, conducting more detailed economic analyses that include dynamic pricing models for hydrogen and electricity could provide insights into how fluctuating market conditions affect system profitability. Incorporating real-time data and forecasting analytics might help optimise the economic performance of power to hydrogen systems under varying market scenarios.

Ultimately, the thesis concludes that a strategic balance between component capacities, operational controls, and market conditions is crucial for optimizing the power to hydrogen system. By leveraging RESs, managing hydrogen production, and selling effectively, the system can achieve significant economic and environmental benefits.

References

[1] Sawle Y, Gupta SC & Kumar Bohre A, "PV-wind hybrid system: A review with case study," *Cogent Engineering*, vol. 3, *(1)*, pp. 1189305, 2016. DOI: 10.1080/23311916.2016.1189305.

[2] Sawle Y, Gupta SC & Bohre AK, "Socio-techno-economic design of hybrid renewable energy system using optimization techniques," *Renewable Energy*, vol. 119, pp. 459-472, 2018. DOI: 10.1016/j.renene.2017.11.058.

[3] Ma T, Yang H, Lu L & Peng J, "Optimal design of an autonomous solar–wind-pumped storage power supply system," *Apply Energy*, vol. 160, pp. 728-736, 2015. DOI: 10.1016/j.apenergy.2014.11.026.

[4] Sinha S & Chandel SS, "Review of recent trends in optimization techniques for solar photovoltaic–wind based hybrid energy systems," *Renewable & Sustainable Energy Reviews*, vol. 50, pp. 755-769, 2015. DOI: 10.1016 /j.rser.2015.05.040.

[5] Gökçek M & Kale C, "Techno-economical evaluation of a hydrogen refuelling station powered by Wind-PV hybrid power system: A case study for İzmir-Çeşme," *Int J Hydrogen Energy*, vol. 43, *(23)*, pp. 10615-10625, 2018. DOI: 10.1016/j.ijhydene.2018.01.082.

[6] Ibáñez-Rioja A, Puranen P, Järvinen L, Kosonen A, Ruuskanen V, Ahola J & Koponen J, "Simulation methodology for an off-grid solar–battery–water electrolyzer plant: Simultaneous optimization of component capacities and system control," *Appl. Energy*, vol. 307, pp. 118157, 2022. DOI: 10.1016 /j.apenergy.2021.118157.

[7] Sorrenti I, Zheng Y, Singlitico A & You S, "Low-carbon and cost-efficient hydrogen optimisation through a grid-connected electrolyser: The case of GreenLab skive," *Renewable & Sustainable Energy Reviews*, vol. 171, pp. 113033, 2023. DOI: 10.1016 /j.rser.2022.113033.

[8] Steffen W, Rockström J, Richardson K, Lenton TM, Folke C, Liverman D, Summerhayes CP, Barnosky AD, Cornell SE, Crucifix M, "Trajectories of the Earth System in the Anthropocene," *Proceedings of the National Academy of Sciences*, vol. 115, *(33)*, pp. 8252-8259, 2018. DOI: 10.1073/pnas.1810141115.

[9] IEA, "*The future of hydrogen," 2019*. Available: https://www.oecd-ilibrary.org /content/publication/1e0514c4-en.

[10] Bogdanov D, Farfan J, Sadovskaia K, Aghahosseini A, Child M, Gulagi A, Oyewo AS, de Souza Noel Simas Barbosa L & Breyer C, "Radical transformation pathway towards sustainable electricity via evolutionary steps," *Nature Communications*, vol. 10, *(1)*, pp. 1077, 2019. DOI: 10.1038/s41467-019-08855-1.

[11] European Commission, *"A clean planet for all. A european long-term strategic vision for a prosperous, modern, competitive and climate neutral economy,"* European Commission, Brussels, 2018. Available: https://climatecooperation.cn /wp-content/uploads/2019/06/com_2018_733_analysis_in_support_en_0.pdf.

[12] Wang T, Tao L, Zhu X, Chen C, Chen W, Du S, Zhou Y, Zhou B, Wang D, Xie C, "Combined anodic and cathodic hydrogen production from aldehyde oxidation and hydrogen evolution reaction," *Nature Catalysis,* vol. 5, 2022. DOI: 10.1038/s41929-021-00721-y.

[13] L. Lin *et al*, "Low-temperature hydrogen production from water and methanol using Pt/α-MoC catalysts," *Nature (London),* vol. 544, *(7648),* pp. 80-83, 2017. DOI: 10.1038/nature21672.

[14] Lin L, Zhou W, Gao R, Yao S, Zhang X, Xu W, Zheng S, Jiang Z, Yu Q, Li Y, "Intermodule Management Within a Large-Capacity High-Temperature Power-to-Hydrogen Plant," *Tec,* vol. 35, *(3),* pp. 1432-1442, 2020. DOI: 10.1109/TEC.2020.2978552.

[15] Qureshy AMMI & Dincer I, "Energy and exergy analyses of an integrated renewable energy system for hydrogen production," *Energy (Oxf.),* vol. 204, pp. 117945, 2020. DOI: 10.1016/j.energy.2020.117945.

[16] Liu J, Zhou F, Abed AM, Le BN, Dai L, Elhosiny Ali H, Khadimallah MA & Zhang G , "Macroalgae as a potential source of biomass for generation of biofuel: Artificial intelligence, challenges, and future insights towards a sustainable environment," *Fuel (Guildford),* vol. 336, pp. 126826, 2023. DOI: 10.1016/j.fuel.2022.126826.

[17] Dincer I & Acar C, "A review on clean energy solutions for better sustainability," *Int. J. Energy Res.,* vol. 39, 2015. DOI: 10.1002/er.3329.

[18] IRENA, *Hydrogen.* Available: https://www.irena.org/Energy Transition/ Technology/Hydrogen.

[19] Hirscher M, Yartys VA, Baricco M, Bellosta von Colbe J, Blanchard D, Bowman RC, Broom DP, Buckley CE, Chang F, Chen P, "Materials for hydrogen-based energy storage – past, recent progress and future outlook," *J. Alloys Compounds,* vol. 827, pp. 153548, 2020. DOI: 10.1016/j.jallcom.2019.153548.

[20] Bauer C, Treyer K, Antonini C, Bergerson J, Gazzani M, Gencer E, Gibbins J, Mazzotti M, McCoy ST, McKenna R, "On the climate impacts of blue hydrogen production," *Sustainable Energy & Fuels,* vol. 6, *(1),* pp. 66-75, 2021. DOI: 10.1039/d1se01508g.

[21] Oliveira AM, Beswick RR & Yan Y, "A green hydrogen economy for a renewable energy society," *Current Opinion in Chemical Engineering,* vol. 33, pp. 100701, 2021. DOI: 10.1016/j.coche.2021.100701.

[22] Nikolaidis P & Poullikkas A, "A comparative overview of hydrogen production processes," *Renewable & Sustainable Energy Reviews,* vol. 67, pp. 597-611, 2017. DOI: 10.1016/j.rser.2016.09.044.

[23] Muradov NZ & Veziroğlu TN, "From hydrocarbon to hydrogen–carbon to hydrogen economy," *Int J Hydrogen Energy,* vol. 30, *(3),* pp. 225-237, 2005. DOI: 10.1016/j.ijhydene.2004.03.033.

[24] Faye O, Szpunar J & Eduok U, "A critical review on the current technologies for the generation, storage, and transportation of hydrogen," *Int J Hydrogen Energy,* vol. 47, *(29),* pp. 13771-13802, 2022. DOI: 10.1016/j.ijhydene.2022.02.112.

[25] Megia PJ, Vizcaíno A, Calles J & Carrero A, "Hydrogen Production Technologies: From Fossil Fuels toward Renewable Sources. A Mini Review," *Energy Fuels,* vol. 35, 2021. DOI: 10.1021/acs.energyfuels.1c02501.

[26] Ursua A, Gandia LM & Sanchis P, "Hydrogen Production From Water Electrolysis: Current Status and Future Trends," *Jproc,* vol. 100, *(2),* pp. 410-426, 2012. DOI: 10.1109/JPROC.2011.2156750.

[27] Chi J & Yu H, "Water electrolysis based on renewable energy for hydrogen production," *Chinese Journal of Catalysis,* vol. 39, *(3),* pp. 390-394, 2018. DOI: 10.1016/S1872-2067(17)62949-8.

[28] FUNK JE, "Thermochemical hydrogen production: past and present," *Int J Hydrogen Energy,* vol. 26, *(3),* pp. 185-190, 2001. DOI: 10.1016/S0360-3199(00)00062-8.

[29] Joya KS, Joya YF, Ocakoglu K & van de Krol R, "Water-Splitting Catalysis and Solar Fuel Devices: Artificial Leaves on the Move," *Angewandte Chemie (International Ed.),* vol. 52, *(40),* pp. 10426-10437, 2013. DOI: 10.1002 /anie.201300136.

[30] IEA, *"Renewables, analysis and forecast 2022 to 2027,"* January. 2023. Available: https://iea.blob.core.windows.net/assets/ada7af90-e280-46c4-a577-df2e4fb44254/Renewables2022.pdf.

[31] IEA, *Total renewable capacity dedicated to hydrogen production in the main and accelerated case globally, 2021-2027.* Available: https://www.iea.org/data-and-statistics/charts/total-renewable-capacity-dedicated-to-hydrogen-production-in-the-main-and-accelerated-case-globally-2021-2027.

[32] IRENA, *"Hydrogen: A renewable energy perspective,"* IRENA, September. 2019. Available: https://www.irena.org/-/media/Files/IRENA/Agency/Publication/2019/Sep/IRENA_Hydrogen_2019.pdf?rev=99c1fc338b5149eb846c0d84d633bccd.

[33] CCS, *"Global status of CCS report: 2020,"* Global CCS Institute, December. 2020. Available:https://www.globalccsinstitute.com/wp-content/uploads/2021/09/Global-Status-of-CCS-Report-Jan-28-1.pdf.

[34] Roussanaly S, "Calculating CO 2 avoidance costs of Carbon Capture and Storage from industry," *Carbon Management,* vol. 10, pp. 1-8, 2019. DOI: 10.1080 /17583004.2018.1553435.

[35] Weidner S, Faltenbacher M, François I, Thomas D, Skùlason JB & Maggi C, "Feasibility study of large scale hydrogen power-to-gas applications and cost of the systems evolving with scaling up in Germany, Belgium and Iceland," *Int J Hydrogen Energy,* vol. 43, *(33),* pp. 15625-15638, 2018. DOI: 10.1016 /j.ijhydene.2018.06.167.

[36] Newborough M & Cooley G, "Developments in the global hydrogen market: The spectrum of hydrogen colours," *Fuel Cells Bulletin,* vol. 2020, *(11),* pp. 16-22, 2020. DOI: 10.1016/S1464-2859(20)30546-0.

[37] Hydrogen Council, *"Path to hydrogen competitiveness, A cost perspective,"* Hydrogen Council, January. 2020. Available: https://hydrogencouncil.com/wp-content/uploads/2020/01/Path-to-Hydrogen-Competitiveness_Full-Study-1.pdf.

[38] Jäger-Waldau A, Kougias I, Taylor N & Thiel C, "How photovoltaics can contribute to GHG emission reductions of 55% in the EU by 2030," *Renewable & Sustainable Energy Reviews,* vol. 126, pp. 109836, 2020. DOI: 10.1016/j.rser.2020.109836.

[39] BloombergNEF, *"Hydrogen economy outlook,"* BloombergNEF, 30 March. 2020. Available: https://data.bloomberglp.com/professional/sites/24/BNEF-Hydrogen-Economy-Outlook-Key-Messages-30-Mar-2020.pdf.

[40] IRENA, *"Renewable power generation costs in 2019,"* IRENA, 2020. Available: https://www.irena.org/-/media/Files/IRENA/Agency/Publication/2020/Jun /IRENA_Power_Generation_Costs_2019.pdf?rev=77ebbae10ca34ef98909a59e39 470906.

[41] Moradpoor I, Syri S & Santasalo-Aarnio A, "Green hydrogen production for oil refining – Finnish case," *Renewable & Sustainable Energy Reviews,* vol. 175, pp. 113159, 2023. DOI: 10.1016/j.rser.2023.113159.

[42] Tang O, Rehme J & Cerin P, "Levelized cost of hydrogen for refueling stations with solar PV and wind in Sweden: On-grid or off-grid?" *Energy (Oxf.),* vol. 241, pp. 122906, 2022. DOI: 10.1016/j.energy.2021.122906.

[43] Business Finland, *"National hydrogen roadmap for Finland,"* Business Finland, November. 2020. Available: https://www.businessfinland.fi/4abb35 /globalassets /Finnish-customers/02-build-your-network/bioeconomy--cleantech/alykas-energia /bf_national_hydrogen_roadmap_2020.pdf.

[44] Koivunen T, Khosravi A & Syri S, "The role of power – to – hydrogen in carbon neutral energy and industrial systems: Case Finland," *Energy (Oxf.)*, vol. 284, pp. 128624, 2023. DOI: 10.1016/j.energy.2023.128624.

[45] Nord Pool 2023, *History*. Available: https://www.nordpoolgroup.com/en/About-us/History/

[46] Soysal ER, Olsen OJ, Skytte K, Sekamane JK, "Intraday market asymmetries - A nordic example," in 2017. DOI: 10.1109/EEM.2017.7981920.

[47] Voronin S, "Price Spike Forecasting in a Competitive Day-Ahead Energy Market." , Lappeenranta University of Technology, Lappeenranta, 2013.

[48] IEA, *"Finland 2023, energy policy review,"* IEA, 2023. Available: https://iea.blob.core.windows.net/assets/842c42c2-8d79-4845-92c8-d36c0ff96ef4/Finland2023-EnergyPolicyReview.pdf.

[49] Finland Statistics, *Production of Electricity*. Available: https://www.stat.fi/en/publication/cl8mo29omxf8t0dukky5aa8i1.

[50] Ember, *Monthly Electricity Data.* Available: https://www-statista-com.ezproxy.cc.lut.fi/statistics/1271437/finland-monthly-wholesale-electricity-price/.

[51] IPCC, "*Climate change 2022 mitigation of climate change,"* IPCC, 2022. Available: https://www.ipcc.ch/report/ar6/wg3/downloads/report/ IPCC_AR6_WGIII_FullReport.pdf.

[52] Galimova T, Ram M, Bogdanov D, Fasihi M, Khalili S, Gulagi A, Karjunen H, Mensah TNO & Breyer C, "Global demand analysis for carbon dioxide as raw material from key industrial sources and direct air capture to produce renewable electricity-based fuels and chemicals," *J. Clean. Prod.,* vol. 373, pp. 133920, 2022. DOI: 10.1016/j.jclepro.2022.133920.

[53] Perera F, "Pollution from Fossil-Fuel Combustion is the Leading Environmental Threat to Global Pediatric Health and Equity: Solutions Exist," *International Journal of Environmental Research and Public Health,* vol. 15, pp. 16, 2017. DOI: 10.3390/ijerph15010016.

[54] Breyer C, Khalili S, Bogdanov D, Ram M, Oyewo AS, Aghahosseini A, Gulagi A, Solomon AA, Keiner D, Lopez G, "On the History and Future of 100% Renewable Energy Systems Research," *Access,* vol. 10, pp. 78176-78218, 2022. DOI: 10.1109/ACCESS.2022.3193402.

[55] Erdiwansyah, Mahidin, Husin H, Nasaruddin, Zaki M & Muhibbuddin, "A critical review of the integration of renewable energy sources with various technologies," *Prot Control Mod Power Syst,* vol. 6, *(1),* pp. 1-18, 2021. DOI: 10.1186/s41601-021-00181-3.

[56] Schill W & Zerrahn A, "Flexible electricity use for heating in markets with renewable energy," *Appl. Energy,* vol. 266, pp. 114571, 2020. DOI: 10.1016 /j.apenergy.2020.114571.

[57] IEA, *"Renewable energy market update outlook for 2023 and 2024,"* IEA, June. 2023. Available: https://iea.blob.core.windows.net/assets/63c14514-6833-4cd8-ac53-f9918c2e4cd9/RenewableEnergyMarketUpdate_June2023.pdf.

[58] European Commission, *"2023 progress report on competitiveness of clean energy technologies,"* European Commission, 2023. Available: https://eur-lex.europa.eu /legal-content/EN/TXT/PDF/?uri=CELEX:52023DC0652.

[59] IEA, *"Offshore wind outlook 2019,"* IEA, 2019. Available: https:// iea.blob.core.windows.net/assets/495ab264-4ddf-4b68-b9c0-514295ff40a7 /Offshore_Wind_Outlook_2019.pdf.

[60] Koutroulis E & Kalaitzakis K, "Design of a maximum power tracking system for wind-energy-conversion applications," *Tie,* vol. 53, *(2),* pp. 486-494, 2006. DOI: 10.1109/TIE.2006.870658.

[61] Wind Europe, *"Wind energy in europe: Scenarios for 2030,"* Wind Europe, September. 2017. Availabel: https://windeurope.org/wp-content/uploads/files /about-wind/reports/Wind-energy-in-Europe-Scenarios-for-2030.pdf.

[62] ITA, *Finland - Country Commercial Guide.* Available: https://www.trade.gov /country-commercial-guides/finland-energy.

[63] IEA Data Services, *Finland*. Availabel: https://www.iea.org/countries/finland /energy-mix.

[64] Finland Statistics, *Total Energy Consumption by Energy Source.* Available: https://pxdata.stat.fi/PxWeb/pxweb/en/StatFin/StatFin__ehk/statfin_ehk_pxt_12v q.px/table/tableViewLayout1/.

[65] Lund H, Østergaard PA, Connolly D & Mathiesen BV, "Smart energy and smart energy systems," *Energy (Oxf.),* vol. 137, pp. 556-565, 2017. DOI: 10.1016 /j.energy.2017.05.123.

[66] Tomsic Z, Rajsl I & Filipovic M, "Model for the techno-economic analysis of common work of wind power and CCGT power plant to offer constant level of power in the electricity market," *E3S Web of Conferences,* vol. 23, pp. 9002, 2017. DOI: 10.1051/e3sconf/20172309002.

[67] Aktaş A & Kırçiçek Y, "A novel optimal energy management strategy for offshore wind/marine current/battery/ultracapacitor hybrid renewable energy system," *Energy (Oxf.),* vol. 199, pp. 117425, 2020. DOI: 10.1016 /j.energy.2020.117425.

[68] Mikulčić H, Ridjan Skov I, Dominković DF, Wan Alwi SR, Manan ZA, Tan R, Duić N, Hidayah Mohamad SN & Wang X, "Flexible Carbon Capture and

Utilization technologies in future energy systems and the utilization pathways of captured CO2," *Renewable & Sustainable Energy Reviews,* vol. 114, pp. 109338, 2019. DOI: 10.1016 /j.rser.2019.109338.

[69] Acar C, "A comprehensive evaluation of energy storage options for better sustainability," *Int. J. Energy Res.,* vol. 42, 2018. DOI: 10.1002/er.4102.

[70] Agata Godula-Jopek, *Hydrogen Production: By Electrolysis.* (1st ed.) 2015. DOI: 10.1002/9783527676507.

[71] Qureshi F, Yusuf M, Arham Khan M, Ibrahim H, Ekeoma BC, Kamyab H, Rahman MM, Nadda AK & Chelliapan S, "A State-of-The-Art Review on the Latest trends in Hydrogen production, storage, and transportation techniques," *Fuel (Guildford),* vol. 340, pp. 127574, 2023. DOI: 10.1016/j.fuel.2023.127574.

[72] Tarkowski R & Uliasz-Misiak B, "Towards underground hydrogen storage: A review of barriers," *Renewable & Sustainable Energy Reviews,* vol. 162, pp. 112451, 2022. DOI: 10.1016/j.rser.2022.112451.

[73] Le TS, Nguyen TN, Bui D & Ngo TD, "Optimal sizing of renewable energy storage: A techno-economic analysis of hydrogen, battery and hybrid systems considering degradation and seasonal storage," *Appl. Energy,* vol. 336, pp. 120817, 2023. DOI: 10.1016 /j.apenergy.2023.120817.

[74] Viteri JP, Viteri S, Alvarez-Vasco C & Henao F, "A systematic review on green hydrogen for off-grid communities –technologies, advantages, and limitations," *Int J Hydrogen Energy,* vol. 48, *(52),* pp. 19751-19771, 2023. DOI: 10.1016 /j.ijhydene.2023.02.078.

[75] Zaghba L, Borni A, Khennane M, Terki N, Fezzani A, Bouchakour A, Mahamed IH & Oudjana SH, "Experimental typical meteorological years to study energy performance of a PV grid-connected system," *Energy Procedia,* vol. 119, pp. 297-307, 2017. DOI: 10.1016/j.egypro.2017.07.085.

[76] Askarzadeh A, "Developing a discrete harmony search algorithm for size optimization of wind–photovoltaic hybrid energy system," *Solar Energy,* vol. 98, pp. 190-195, 2013. DOI: 10.1016/j.solener.2013.10.008.

[77] Zhou W, Lou C, Li Z, Lu L & Yang H, "Current status of research on optimum sizing of stand-alone hybrid solar–wind power generation systems," *Appl. Energy,* vol. 87, *(2),* pp. 380-389, 2010. DOI: 10.1016/j.apenergy.2009.08.012.

[78] Hassan Q, Abdulateef AM, Hafedh SA, Al-samari A, Abdulateef J, Sameen AZ, Salman HM, Al-Jiboory A, Wieteska S & Jaszczur M, "Renewable energy-to-green hydrogen: A review of main resources routes, processes and evaluation," *Int J Hydrogen Energy,* vol. 48, *(46),* pp. 17383-17408, 2023. DOI: 10.1016 /j.ijhydene.2023.01.175.

[79] Hofrichter A, Rank D, Heberl M & Sterner M, "Determination of the optimal power ratio between electrolysis and renewable energy to investigate the effects on the hydrogen production costs," *Int J Hydrogen Energy,* vol. 48, *(5),* pp. 1651-1663, 2023. DOI: 10.1016 /j.ijhydene.2022.09.263.

[80] Scolaro M & Kittner N, "Optimizing hybrid offshore wind farms for cost-competitive hydrogen production in Germany," *Int J Hydrogen Energy,* vol. 47, *(10),* pp. 6478-6493, 2022. DOI: 10.1016/j.ijhydene.2021.12.062.

[81] Tang O, Rehme J & Cerin P, "Levelized cost of hydrogen for refueling stations with solar PV and wind in Sweden: On-grid or off-grid?" *Energy (Oxf.),* vol. 241, pp. 122906, 2022. DOI: 10.1016/j.energy.2021.122906.

[82] Scheepers F, Stähler M, Stähler A, Müller M & Lehnert W, "Cost-optimized design point and operating strategy of polymer electrolyte membrane electrolyzers," *Int J Hydrogen Energy,* vol. 48, *(33),* pp. 12185-12199, 2023. DOI: 10.1016 /j.ijhydene.2022.11.288.

[83] María Villarreal Vives A, Wang R, Roy S & Smallbone A, "Techno-economic analysis of large-scale green hydrogen production and storage," *Appl. Energy,* vol. 346, pp. 121333, 2023. DOI: 10.1016/j.apenergy.2023.121333.

[84] Das BK, Hasan M & Das P, "Impact of storage technologies, temporal resolution, and PV tracking on stand-alone hybrid renewable energy for an Australian remote area application," *Renewable Energy,* vol. 173, pp. 362-380, 2021. DOI: 10.1016 /j.renene.2021.03.131.

[85] Marocco P, Gandiglio M & Santarelli M, "Optimal design of PV-based grid-connected hydrogen production systems," *J. Clean. Prod.,* vol. 434, pp. 140007, 2024. DOI: 10.1016/j.jclepro.2023.140007.

[86] Park J, Hwan Ryu K, Kim C, Chul Cho W, Kim M, Hun Lee J, Cho H & Lee JH, "Green hydrogen to tackle the power curtailment: Meteorological data-based capacity factor and techno-economic analysis," *Appl. Energy,* vol. 340, pp. 121016, 2023. DOI: 10.1016/j.apenergy.2023.121016.

[87] Wankouo Ngouleu CA, Koholé YW, Fohagui FCV & Tchuen G, "Techno-economic analysis and optimal sizing of a battery-based and hydrogen-based standalone photovoltaic/wind hybrid system for rural electrification in Cameroon based on meta-heuristic techniques," *Energy Conversion and Management,* vol. 280, pp. 116794, 2023. DOI: 10.1016 /j.enconman.2023.116794.

[88] Babaei R, Ting DS- & Carriveau R, "Optimization of hydrogen-producing sustainable island microgrids," *Int J Hydrogen Energy,* vol. 47, *(32),* pp. 14375-14392, 2022. DOI: 10.1016/j.ijhydene.2022.02.187.

[89] Fragiacomo P & Genovese M, "Technical-economic analysis of a hydrogen production facility for power-to-gas and hydrogen mobility under different

renewable sources in Southern Italy," *Energy Conversion and Management,* vol. 223, pp. 113332, 2020. DOI: 10.1016/j.enconman.2020.113332.

[90] Wankouo Ngouleu CA, Koholé YW, Fohagui FCV & Tchuen G, "Techno-economic analysis and optimal sizing of a battery-based and hydrogen-based standalone photovoltaic/wind hybrid system for rural electrification in Cameroon based on meta-heuristic techniques," *Energy Conversion and Management,* vol. 280, pp. 116794, 2023. DOI: 10.1016 /j.enconman.2023.116794.

[91] Wang J, Xu X, Wu L, Huang Q, Chen Z & Hu W, "Risk-averse based optimal operational strategy of grid-connected photovoltaic/wind/battery/diesel hybrid energy system in the electricity/hydrogen markets," *Int J Hydrogen Energy,* vol. 48, *(12),* pp. 4631-4648, 2023. DOI: 10.1016/j.ijhydene.2022.11.006.

[92] Park J, Hwan Ryu K, Kim C, Chul Cho W, Kim M, Hun Lee J, Cho H & Lee JH, "Green hydrogen to tackle the power curtailment: Meteorological data-based capacity factor and techno-economic analysis," *Appl. Energy,* vol. 340, pp. 121016, 2023. DOI: 10.1016/j.apenergy.2023.121016.

[93] Khater HA, Abdelraouf AA & Beshr MH, "Optimum Alkaline Electrolyzer-Proton Exchange Membrane Fuel Cell Coupling in a Residential Solar Stand-Alone Power System," *ISRN Renewable Energy,* vol. 2011, pp. 1-13, 2011. DOI: 10.5402 /2011/953434.

[94] Micena RP, Llerena-Pizarro O, de Souza TM & Silveira JL, "Solar-powered Hydrogen Refueling Stations: A techno-economic analysis," *Int J Hydrogen Energy,* vol. 45, *(3),* pp. 2308-2318, 2020. DOI: 10.1016/j.ijhydene.2019.11.092.

[95] Zare Oskouei Morteza, Mohammadi-Ivatloo Behnam, Erdinç Ozan, Gülsen Erdinç Fatma, "Multi-objective risk-constrained operation of hydrogen-based renewable energy integrated distribution network," *Wiley,* pp. 7-8, 2022. DOI: 10.1002/er.8172.

[96] Jafari M, Armaghan D, Seyed Mahmoudi SM & Chitsaz A, "Thermoeconomic analysis of a standalone solar hydrogen system with hybrid energy storage," *Int J Hydrogen Energy,* vol. 44, *(36),* pp. 19614-19627, 2019. DOI: 10.1016 /j.ijhydene.2019.05.195.

[97] Seyfi M, Mehdinejad M, Mohammadi-Ivatloo B & Shayanfar H, "Scenario-based robust energy management of CCHP-based virtual energy hub for participating in multiple energy and reserve markets," *Sustainable Cities and Society,* vol. 80, pp. 103711, 2022. DOI: 10.1016/j.scs.2022.103711.

[98] IEA, *"Global hydrogen review 2023,"* 2023. Available: https: //iea.blob.core. windows.net/assets/ecdfc3bb-d212-4a4c-9ff7-6ce5b1e19cef /GlobalHydrogenReview2023.pdf.

[99] Lehmann J, Wabbes A, Miguelañez Gonzalez E & Scheerlinck S, "Levelized Cost of Hydrogen Calculation from Off-Grid Photovoltaic Plants Using Different Methods," *Solar RRL*, vol. 6, *(5)*, pp. n/a, 2022. DOI: 10.1002/solr.202100482.

[100] Finnish Meteorological Institute, *Meteorological Data*. Available: https:// en.ilmatieteenlaitos.fi/download-observations.

[101] ENTSOE, *Hourly Electricity Prices*. Available: https://transparency.entsoe.eu /transmission-domain/r2/dayAheadPrices/show?name=&defaultValue =true&viewType=TABLE&areaType=BZN&atch=false&dateTime.dateTime=01. 01.2023+00:00|EET|DAY&biddingZone.values=CTY|10YFI-1-U!BZN|10YFI-1-U&resolution.values=PT60M&dateTime.timezone=EET_EEST&dateTime.timezone_input =EET+(UTC+2)+/+EEST+(UTC+3).

[102] IRENA, *"Renewable power generation cost in 2022,"* 2023. Available: https://mc-cd8320d4-36a1-40ac-83cc-3389-cdn-endpoint.azureedge.net/-/media/Files/IRENA/Agency/Publication/2023/Aug/IRENA_Renewable_power_generation_costs_in_2022.pdf?rev=cccb713bf8294cc5bec3f870e1fa15c2.

[103] Vestas, *EnVentus Platform Brochure*. Available: https:// nozebra .ipapercms.dk /Vestas/Communication/Productbrochure/enventus/enventus-platform-brochure/.

[104] Global Wind Atlas, *Kannus Wind Farm*. Available: https://globalwindatlas.info/en.

[105] Danish Energy Agency, *"Technology data - energy plants for electricity and district heating generation,"* 2024. Available: https://ens.dk/sites/ens.dk/files /Analyser /technology_data_catalogue_for_el_and_dh.pdf.

[106] Nordenergi, *"Nordic tax report 2023 electricity sector,"* Nordenergi WG Taxes and Levies, 2023. Available: https://www.energiforetagen.se/4a0314/globalassets /dokument/nordenergi/sk-21-nordenergi-tax-2023-final.pdf.

[107] European Environment Agency, *Greenhouse gas emission intensity of electricity generation in Europe*. Available: https://www.eea.europa.eu/en/analysis/indicators /greenhouse-gas-emission-intensity-of-1.

[108] Hydrogen Europe, *"Clean hydrogen monitor ,"* 2023. Available: https:// hydrogeneurope.eu/wp- content/uploads/2023/10/Clean_Hydrogen_Monitor_11-2023_DIGITAL.pdf.

[109] Oxford Institute for Energy Studies, *"Cost-competitive green hydrogen: How to lower the cost of electrolysers?"* 2022. Available: https:// www.oxfordenergy.org /wpcms/wp-content/uploads/2022/01/Cost-competitive-green-hydrogen-how-to-lower-the-cost-of-electrolysers-EL47.pdf.

[110] Buttler A & Spliethoff H, "Current status of water electrolysis for energy storage, grid balancing and sector coupling via power-to-gas and power-to-liquids: A review," *Renewable & Sustainable Energy Reviews,* vol. 82, pp. 2440-2454, 2018. DOI: 10.1016/j.rser.2017.09.003.

[111] Danish Energy Agency, *"Technology data – renewable fuels,"* 2024. Available: https://ens.dk/sites/ens.dk/files/Analyser/technology_data_for_renewable_fuels.pdf.

[112] Luo Y, Shi Y & Cai N, "Bridging a bi-directional connection between electricity and fuels in hybrid multienergy systems," in Anonymous 2020.

[113] Cruz-Soto J, Azkona-Bedia I, Velazquez-Limon N & Romero-Castanon T, "A techno-economic study for a hydrogen storage system in a microgrid located in baja California, Mexico. Levelized cost of energy for power to gas to power scenarios," *Int J Hydrogen Energy,* vol. 47, *(70),* pp. 30050-30061, 2022. DOI: 10.1016 /j.ijhydene.2022.03.026.

[114] Marocco P, Ferrero D, Martelli E, Santarelli M & Lanzini A, "An MILP approach for the optimal design of renewable battery-hydrogen energy systems for off-grid insular communities," *Energy Conversion and Management,* vol. 245, pp. 114564, 2021. DOI: 10.1016 /j.enconman.2021 .114564.

[115] Marocco P, Gandiglio M & Santarelli M, "When SOFC-based cogeneration systems become convenient? A cost-optimal analysis," *Energy Reports,* vol. 8, pp. 8709-8721, 2022. Available: https://www.sciencedirect.com/science/article/pii /S2352484722011556. DOI: 10.1016/j.egyr.2022.06.015.

[116] Xu X, Hu W, Cao D, Huang Q, Liu Z, Liu W, Chen Z & Blaabjerg F, "Scheduling of wind-battery hybrid system in the electricity market using distributionally robust optimization," *Renewable Energy,* vol. 156, pp. 47-56, 2020. DOI: 10.1016 /j.renene.2020.04.057.

[117] National Renewable Energy Laboratory, *"Cost projections for utility-scale battery storage: 2021 update,"* 2021. Available: https://www.nrel.gov/docs /fy21osti/79236.pdf.

[118] Danish Energy Agency, *"Technology data – energy storage,"* 2020. Available: https://ens.dk/sites/ens.dk/files/Analyser/technology_data_catalogue_for_energy_storage. pdf.

[119] Marocco P, Gandiglio M, Audisio D & Santarelli M, "Assessment of the role of hydrogen to produce high-temperature heat in the steel industry," *J. Clean. Prod.,* vol. 388, pp. 135969, 2023. DOI: 10.1016/j.jclepro.2023.135969.

[120] Hai T, Kumar A, Aminian S, Mahariq I, Sillanpää M, Fouad H & El-Shafai W, "Transient multi-objective optimization of solar and fuel cell power generation systems with hydrogen storage for peak-shaving applications," *Int J Hydrogen Energy,* vol. 64, pp. 220-235, 2024. DOI: 10.1016 /j.ijhydene.2024.02.282.